POLITECNICO DI TORINO

MASTER's Degree in ELECTRONIC ENGINEERING

MASTER's Degree Thesis

Wireless sensor based on SAW device: Mathematical Modelling, Manufacturing process and testing

Supervisors

Prof. MATTEO COCUZZA

PhD ALESSIO VERNA

Candidate

LORENZO MARIA SCARRONE

MONTH 2021

Summary

The purpose of this text is to provide the reader with a fair number of elements to understand what a SAW (Surface Acoustic Wave) device is and what its possible applications are, in particular to analyze the specific case of wireless sensors.The second chapter presents some of the most significant mathematical models for describing the behaviour of SAW devices.Then is analyzed the development of a transponder model based on a Two-Port SAW resonator, to read a commercial PT100 temperature sensor. The device is made by photolithography on a substrate of $LiNbO_3$ and then characterized through the use of a Vector Network Analyzer (NanoVNA). Finally, some considerations are made about wireless measurements.

Acknowledgements

Throughout the writing of this dissertation I have received a great deal of support and assistance.

I would like to acknowledge the Politecnico di Torino and SMLAB, with particular regard to Roberto Mo and Roberto Pala, who supported me through a scholarship that gave me the opportunity to focus and develop this work.

I would like to acknowledge my supervisor, Professor Matteo Cocuzza who provided me with ideas and research material to develop this project; furthermore he has corrected and revised this dissertation.

I would like to acknowledge my tutor, researcher Alessio Verna, who instructed me on the use of laboratory equipment, helped me to realize the device after two weeks of work.

I would like to thank my family for the hard support who they gave to me in these years, my girlfriend Martina, who bears me and sustained me every day, particularly in these last month, to my friend and colleague Federico who helped me in these years of university.

I would like to thank my friends who are here today to sustain me.

"Thanks to all"

Scarrone Lorenzo Maria

Table of Contents

List of Tables VIII

List of Figures IX

Acronyms XIII

1 Introduction to SAW devices 1
- 1.1 SAW device principles . . . 1
- 1.2 Surface acoustic wave (SAW) . . . 4
- 1.3 SAW transducers (IDT) . . . 7
- 1.4 SAW Delay Line . . . 9
- 1.5 One-Port SAW resonator . . . 10
- 1.6 Two-Port SAW resonator . . . 11

2 Mathematical models 12
- 2.1 Delta function model . . . 13
- 2.2 SAW crossed-field model . . . 17
- 2.3 Equivalent circuit model . . . 23
- 2.4 Matrix building blocks . . . 27
  - 2.4.1 Transmission matrix model . . . 27

3 Device modelling 35

4 Device Realization 46

5 Device testing 55
- 5.1 8 fingers pairs at INPUT and 8 finger pairs at OUTPUT . . . 57
- 5.2 15 fingers pairs at INPUT and 8 finger pairs at OUTPUT . . . 58
- 5.3 15 fingers pairs at INPUT and 15 finger pairs at OUTPUT . . . 59
- 5.4 40 fingers pairs at INPUT and 15 finger pairs at OUTPUT . . . 61
- 5.5 50 fingers pairs at INPUT and 15 finger pairs at OUTPUT . . . 62

5.6 Conclusions 63

6 Testing sensor-transponder configuration 64
6.1 Linear approximation 67
6.2 Quadratic approximation 68
6.3 Conclusions 69

A Matematical models 71
A.1 Delta function model 71

B Source code 74

Bibliography 92

List of Tables

2.1 Material parameters table [11] 25
2.2 Measured characteristic of some Rayleigh-wave Reflection grating types, extracted table from Table 11.2 [13] 31

3.1 Summary of devices 40

4.1 Summary of devices 46

5.1 Summary of tested devices 56

6.1 Measurement summary 66

List of Figures

1.1 Interaction scheme between SAW device and interrogation unit . . 2
1.2 Behaviour of an ID-tag realized on a SAW device 3
1.3 Behaviour of RF response of a solicited ID-tag realized on a SAW device, the long delay line gives the time to dissipate all environmental echoes and obtain a clear sensor response [2] 4
1.4 (a) Atoms displacement due to the propagation of a Rayleigh SAW wave (b) Atoms displacement due to the propagation of a SH-SAW [4] 5
1.5 A travelling SAW wave on a piezoelectric surface, in which is shown that SAW amplitude decays with the depth into the substrate along y-axis[3] 7
1.6 Generic IDT with its constitutive parameters 7
1.7 (a) single-electrode, (b) double-electrode.[5] 8
1.8 Delay line schematic and time response[5] 9
1.9 One-Port SAW resonator 10
1.10 Two-Port SAW resonator schematic 11

2.1 Delta function model applied to an IDT[9] 13
2.2 Definition of the reference plane to apply the delta function model[9] 14
2.3 The frequency response of an IDT obtained with the delta function model[9] 16
2.4 (a) Representation of a SAW IDT as a three-port network, Port 1 and 2 are "acoustic" ports while Port 3 is the electrical one. (b) In the crossed-field model Port 1 and 2 are converted into an equivalent electrical transmission line[9] 17
2.5 Mason's equivalent circuit model 18
2.6 Admittance equivalent circuit model[10] 19
2.7 Crossed-field equivalent admittance at electrical Port 3, for an IDT at center frequency. Conductance $G_a(f)$ relates power generation from an excited IDT. (Analogous to radiation resistance in an electromagnetic antenna) C_T is the total static capacitance of IDT.[10] 21

2.8 Complete model for a SAW device[10] 22
2.9 Generalized electrical model for an IDT finger[11] 23
2.10 ABCD matrix transmission line[11] 25
2.11 The SAW reference planes at i-th element of a SAW reflection grating of length L[12] 29
2.12 Incident SAW on a SAW reflection grating of length L[12] 30
2.13 Reference planes at offsets $\lambda/8 = \Lambda/4$, as used before for an IDT, together with acoustic and electrical ports.[12] 31

3.1 Definition of the IDT structure and constitutive parameters 36
3.2 Layout of the generic Two-Port SAW resonator 37
3.3 Device block schematic[12] 38
3.4 Input/Output relations 8 finger pairs at input 8 finger pairs at output 41
3.5 Input/Output relations 15 finger pairs at input 15 finger pairs at output 42
3.6 Input/Output relations 15 finger pairs at input 8 finger pairs at output 43
3.7 Input/Output relations 40 finger pairs at input 15 finger pairs at output 44
3.8 Input/Output relations 50 finger pairs at input 15 finger pairs at output 45

4.1 "IDT MASK ELEMENT GENERATOR" program. Through this interface, it is possible to generate a SAW device by setting the working frequency, the number of finger pairs in input and output, etc.... It is also possible to set the sequence order of the elements in the "Device structure" field 47
4.2 MASK layout, with the horizontal flat band for the mask alignment 48
4.3 Negative MASK layout 48
4.4 Laser writer: writing on the mask 49
4.5 Mask after chrome etching, on the bottom is present the flat band to align the mask and wafer during the exposure process 49
4.6 Spinning process 50
4.7 UV exposure machine on the left, and mask positioning on the right 51
4.8 Device checking features 51
4.9 Evaporation chamber with melting pot containing aluminum 52
4.10 High Vacuum Evaporator 52
4.11 Evaporator support 53
4.12 (a) the wafer surface after the metal deposition, (b) metallized wafer 53
4.13 Liftoff process 54
4.14 Wafer final result 54

5.1 (a) container closed with contact screws , (b) compartment that contains the SAW device 55
5.2 Connection between NanoVNA and a SAW device 56
5.3 S_{21} : comparison between simulation and real devices 57
5.4 (a) device 1 , -6.54 dB at resonance 99.2MHz , (b) device 4 , -10.98dB dB at resonance 98.9MHz 58
5.5 S_{21} dB response of device 1 compared with the simulation. At resonance device 1 shows an attenuation of -9.56 dB (99.2MHz) meanwhile the simulated one -4.59 dB (100MHz) 59
5.6 S_{21} dB response of devices 2,3,4 compared with the simulation. At resonance (99.2MHz) S_{21} for devices 3,4 is -3.98 dB, for device 4 is -11.48 dB and the simulated one is -3.79 dB (resonance 100MHz) . 60
5.7 S_{21} dB response of device 1. At resonance (99.2 MHz) S_{21} is -10.81 dB 60
5.8 S_{21} response of device 1 and device 2 61
5.9 S_{21} response of device 2 and device 3 and 4 62
5.10 (a) POGO pin: gold plated copper (b) container lid with POGO pins 63

6.1 SAW transponder connected with the sensor 64
6.2 Sensing system: PT100, SAW transponder and NanoVNA 65
6.3 Measured characteristic on temperature change 66
6.4 The two $RL(T)$ approximated characteristics on temperature change 67
6.5 Approximated characteristic on temperature change 68
6.6 Received power from SAW transponder after an interrogation. The power is measured in dBm, $1dB = 10 \cdot \log(1W/1mW) = 30dBm$ . . 70

Acronyms

BW

Bandwidth

COM

Coupling of modes

DUT

Device Under Test

IDT

Interdigital transducer

MEMS

Microelectromechanical systems

RF

Radio frequency

SAW

Surface Acoustic Wave

SH-SAW

Shear Horizontal - Surface Acoustic Wave

STW-SAW

Surface Transverse Wave - Surface Acoustic Wave

RL

Return Loss

RCS

Radar cross-section

Chapter 1

Introduction to SAW devices

1.1 SAW device principles

SAW (Surface Acoustic Wave) devices belong to the class of MEMS (Microelectromechanical Systems) devices. These types of devices exploit the physical properties of various types of materials to employ mechanical functions at the micrometric scale. Nowadays, an enormous amount of these devices can be found in every electronic application such as oscillators, delay lines, sensors, filters, accelerometers and similar.
SAW devices are implemented on piezoelectric substrates in different fields from wireless applications to the simple quartz-oscillator. Due to their small size and endurance, they have been implemented in a wide part of wireless sensing applications and for identification systems often where the environment is inaccessible and inhospitable.
Surface acoustic wave filters currently are implemented in a key role in consumer and communication systems due to their high performances, size and reproducibility. These properties also make them attractive for sensor applications, additionally, SAW devices are already used for passive wireless identification systems (ID-tags). Combining conventional oscillators based on SAW technology and wireless ID-tags system, it is possible to realize remote passive sensors.
There are two ways to realize this kind of sensor: the first is using the substrate surface as a sensing system, the second one consists in using the SAW device only as a passive transponder unit connected to an external sensor. The last one leaves a degree of freedom for the final user to choose directly the physical quantity that

has to be measured.
The main advantages of using these tools as sensors are related to the possibility to get a high performance and maintenance free devices (they do not involve the use of batteries). This permits to install them in unreachable locations (like moving or rotating parts, hazardous environments such as contaminated or high voltage areas or all those places where the use of conventional sensors is complicated or dangerous or expensive) and the possibility to get their response through wireless communication.
In a SAW sensor the physical or chemical quantity, that has to be detected, changes the characteristic propagation of the SAW by acting on surface properties or changing the reflection coefficient of an IDT connected to an external sensor.
A passive wireless SAW sensing system consists of passive SAW sensor devices and an interrogation unit which broadcasts a burst signal to the sensors and processes their responses.

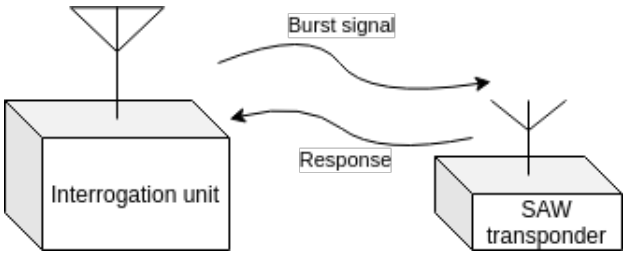

Figure 1.1: Interaction scheme between SAW device and interrogation unit

When an external high frequency signal excitation is applied to the SAW device the interdigital transducer IDT, which is connected to the source of the applied signal, produces a SAW waveform on the material surface. This phenomenon is described in the experiment conducted by White and Voltmer in 1965 on the first engineering application of SAW devices on a planar piezoelectric substrate [1].

The use of ID tags was mentioned earlier and now it is used to introduce the working principle of a SAW sensor device. Looking at the figure 1.2, the incoming RF signal is converted in a SAW propagating on the crystal surface towards the reflectors. The reflectors are placed in a specific barcode-like pattern that reflects part of the incoming wave to the input transducer.

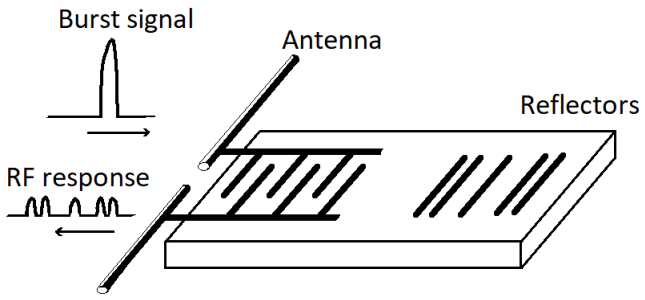

Figure 1.2: Behaviour of an ID-tag realized on a SAW device

What returns to the input IDT is a high frequency series of echoes, which is converted back into an electromagnetic signal. This is the response that is sent through the antenna back to the interrogation unit. The RF response carries the information about the location, the distance between the interrogation unit and the device, while the reflection patterns carry the ID information. One of these reflectors could be another IDT connected to an external sensor. Changing the admittance of the load, also changes the reflection coefficient of the IDT. If there is no external sensor, the SAW can be directly perturbed by the measurand that acts on the material surface. Through the interrogation unit is possible to measure the amplitude, frequency, and time of the signal back and determine the ID and retrieve the sensor reading.
Another advantage of these devices is related to the SAW velocity: the transduction of the electromagnetic field into an acoustic wave permits a long delay time, giving the time to dissipate all environmental echoes given by the interrogation unit. This is possible because the SAW velocity is about five orders of magnitude less than the light-speed. The Delay time of a traveling SAW is defined as

$$\tau = \frac{L}{v_0} \tag{1.1}$$

where L is the distance between input and output IDTs or reflectors and v_0 represents the SAW propagation velocity.

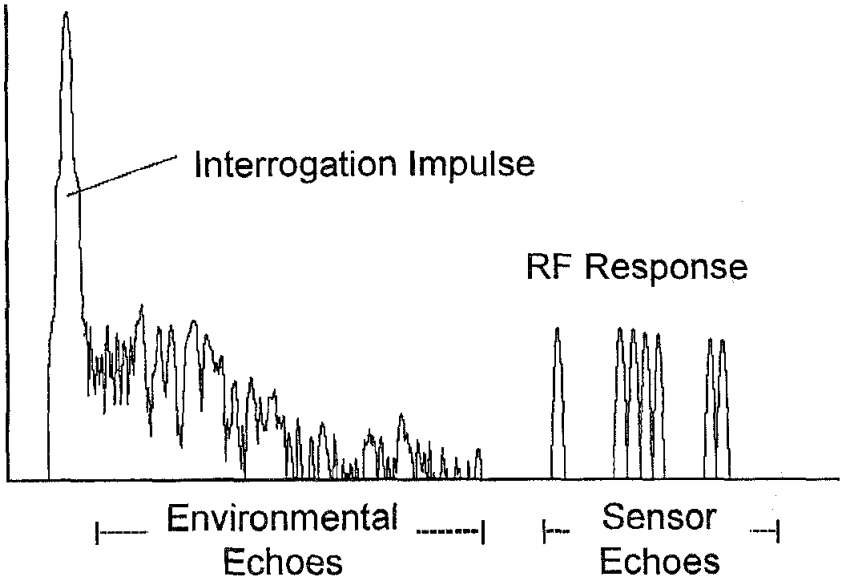

Figure 1.3: Behaviour of RF response of a solicited ID-tag realized on a SAW device, the long delay line gives the time to dissipate all environmental echoes and obtain a clear sensor response [2]

Reading a SAW sensor generally requires only a few microseconds (the time spent by the acoustic wave to travel across the device and back to the input IDT), so many interrogations can be performed in a second (up to 10^5) [2]. This allows the interrogation of fast-moving objects and if the distance between the interrogation unit and SAW transponder is unknown, it is possible to use only differences in amplitude, time and frequency or phase of the RF signal to determine the aimed values.

1.2 Surface acoustic wave (SAW)

A surface acoustic wave (SAW) is a wave which travels along a material surface that exhibits elasticity, the amplitude decays with depth into the substrate material. An interdigitated transducer (IDT) can excite an acoustic wave on a piezoelectric material surface (by converting an electrical signal into a SAW and vice versa) and operates both as an emitter as well as a receiver[1].
If a piezoelectric material is solicited by an applied voltage, it can modify the equilibrium position of its atoms, and this displacement phenomena is called strain. Due to the strain, material generates internal forces which act to return atoms to their equilibrium state. This phenomena is called stress. When a SAW wave is generated both stress and strain are involved as it is a propagating phenomenon

[3].
It is possible to distinguish different waveforms in a SAW device: bulk waves, SAW and pseudo-SAW (or leaky SAW). A bulk wave propagates below the material surface, SAW and pseudo-SAW are, basically, of two types: longitudinal waves and transverse waves. The wave in which atom displacement is parallel to the propagating direction is a longitudinal wave if the displacement occurs in any direction parallel to the wave front is a transverse wave, the last type is known also as shear wave. The difference between a SAW and a pseudo-SAW can be found in the confinement of the energy at the boundary of a piezoelectric surface and a fluid or gas near the surface. In a SAW (or Rayleigh wave) the most of the energy remains confined within a few wavelengths' depth of the substrate, while in a pseudo-SAW some of the same energy is dissipated in into the material near the surface. The wave velocity is determined by the piezoelectric substrate used and the crystal orientation. The periodicity of the IDT fingers determines the frequency of the wave.
In a shear horizontal (SH-) SAW wave the particle displacement is parallel to the sensing surface and normal to the wave propagation direction. In the SH-SAW device, a thin solid film (called Love Wave Device) or grating (called Surface Transverse Wave (STW) Device) are sometimes added to prevent wave diffraction into the bulk. The separation of the IDT fingers and the orientation of the substrate determine the operating frequency.

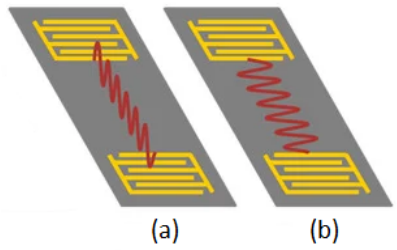

Figure 1.4: (a) Atoms displacement due to the propagation of a Rayleigh SAW wave (b) Atoms displacement due to the propagation of a SH-SAW [4]

For measurements such as viscosity or mass loading of an adjacent liquid is preferred to use the perturbation of the SH-SAW because a large attenuation loss is observed in Rayleigh devices caused by the particle displacement perpendicular to the surface, which generates compression waves radiating into the liquid (leaky SAW).[4]

The action of the electric field, stress and strain can be described by the following two equations[3]:

$$\begin{aligned} [T] &= [e][S] + [\epsilon]\vec{E} \\ \vec{D} &= [c][S] - [\epsilon^t]\vec{E} \end{aligned} \tag{1.2}$$

Where $[T]$ represents the stress and $[S]$ the strain, $\vec{E}$ the applied electric field and $\vec{D}$ the charge displacement due to strain and electric field. $[e]$ is the piezoelectric matrix, $[c]$ is the Young modulus matrix and $[\epsilon]$ is the dielectric constant of the piezoelectric material.
One of the most important parameters that can be derived from the equations (1.2) is the electromechanical coupling coefficient K^2. This value represents a measure of the efficiency of a given piezoelectric material in converting an applied electrical signal into mechanical energy associated with a SAW wave. K^2 can be defined in terms of the piezoelectric coefficient, elastic constant and dielectric permittivity as [3].

$$K^2 = \frac{e^2}{c\epsilon} \tag{1.3}$$

This parameter could also be found experimentally by measuring the ratio between the perturbed velocity on a surface covered by a metal film and the unperturbed velocity[3]:

$$K^2 = -\frac{2\Delta v}{v} \tag{1.4}$$

Rayleigh wave (true-SAW) propagation involves both mechanical motion as well the electromagnetic one; but due to the large difference between the speed of light and the mechanical wave (about five orders of magnitude) it is possible to state that mechanical motion will dominate [3].
So, the wave solution for the mechanical wave propagation at the surface are described only by an electrical potential ϕ produced by charge displacement and a real particle displacement U:

$$\begin{aligned} \phi(x,t) &\approx |\phi| \exp j(\omega t - \beta x - \beta|y|) \\ U(x,t) &\approx |U| \exp j(\omega t - \beta x - \beta|y|) \end{aligned} \tag{1.5}$$

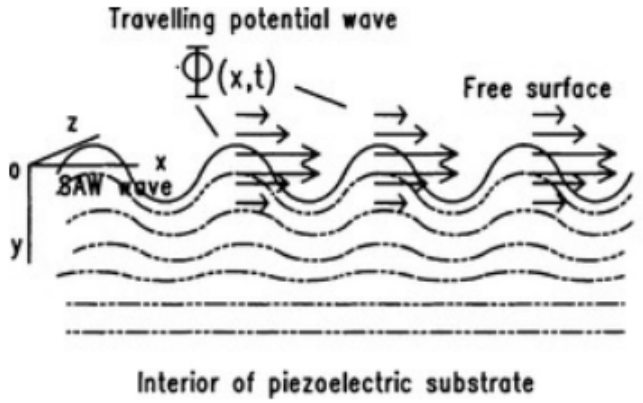

Figure 1.5: A travelling SAW wave on a piezoelectric surface, in which is shown that SAW amplitude decays with the depth into the substrate along y-axis[3]

1.3 SAW transducers (IDT)

The interdigital transducer is the key element in a surface acoustic wave device. The IDT is a source used to generate and receive SAW waves. It is made of a sequence of metal electrodes which consists mainly of aluminum and connected to two bus bars which carry the electrical signal to the IDT fingers.

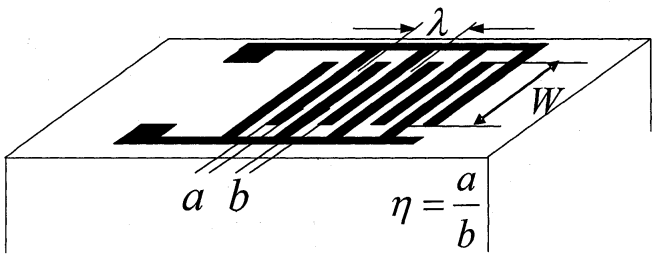

Figure 1.6: Generic IDT with its constitutive parameters

The parameters sketched in the figure 1.6 can be summarized as follows:

W is the acoustic aperture, also known as apodization width. This dimension can be fixed to a static value or vary in the space to shape the frequency response of the element. η is the metallization ratio,that is the ratio between the finger width a and the finger spacing b.

Basically, IDT is a three-port device which has 1 electric port and 2 acoustic ports.

Every time an electric signal is applied to the electrical port, two SAW waves are generated at both acoustic ports and vice versa (when a SAW wave is applied to one the acoustic port a voltage appears on the electric port of the device).
For each IDT it is possible to have different structures according to the different characteristics they have. These characteristics may be differing according to the geometry, fabrication properties, frequency varying factors, etc. Here will be presented two different IDT structures which differ each other on their geometry, phase angle and wavelength. These two are called 'single-electrode IDT' or 'bi-directional IDT' and 'double-electrode IDT' or 'split-electrode IDT'. In the case of 'single-electrode' there is a uniform spacing between fingers $b = \lambda_0/2$. This structure is affected by internal reflections that take place at the center frequency of the IDT $f_0 = v_{saw}/\lambda_0$, which introduce high insertion losses; due to this structure is also called reflective transducer. In the other case, 'double-electrode', each finger is divided into two elements, the electrode pitch becomes $b = \lambda_0/4$. This is called non reflective transducers because the internal reflection phenomenon is shifted at the double of the center frequency.[5][6]

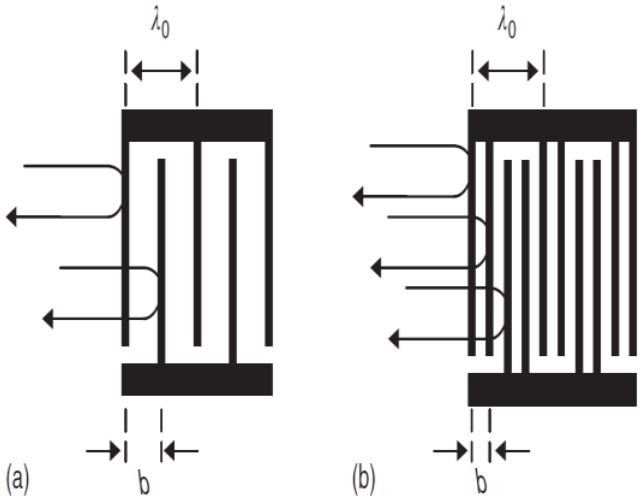

Figure 1.7: (a) single-electrode, (b) double-electrode.[5]

In order to explain the internal reflection phenomenon, it is necessary to recall the Bragg Law, which is involved into wave diffraction in a periodic structure [6][7]

$$2 \cdot d \cdot \sin(\theta) = n \cdot \lambda \Rightarrow \omega_B = \frac{n \cdot \pi \cdot v}{d \cdot \sin(\theta)} \tag{1.6}$$

Where θ is the incident angle of the incoming wave, n is the wave number, d is the element's periodicity and λ is the wavelength of the incident wave. An incident

SAW wave to an IDT has $\theta = 90°$, $n = 1$:

$$\omega_B = \frac{\pi v_{saw}}{d} \iff \lambda = v_{saw}/f_0 \tag{1.7}$$

for a 'single electrode' IDT, $d = \lambda/2$ and the interference occurs at

$$f_B = f0 \tag{1.8}$$

Meanwhile, for a 'double electrode' IDT, $d = \lambda/4$ so

$$f_B = 2f0 \tag{1.9}$$

1.4 SAW Delay Line

In SAW devices an electrical delay is implemented by an acoustic propagation length and the frequency of the delayed signal is chosen according to the geometry and the period of the IDT electrodes. Since the propagation of SAW wave is slower than an electromagnetic wave, it can delay an electrical signal up to several tens of μs, which corresponds to a few km of an electromagnetic wave propagation. The delay can be evaluated considering the SAW velocity and the length of the acoustic line [5]:

$$\tau = \frac{L}{v_{saw}} \tag{1.10}$$

as sketched in figure 1.8:

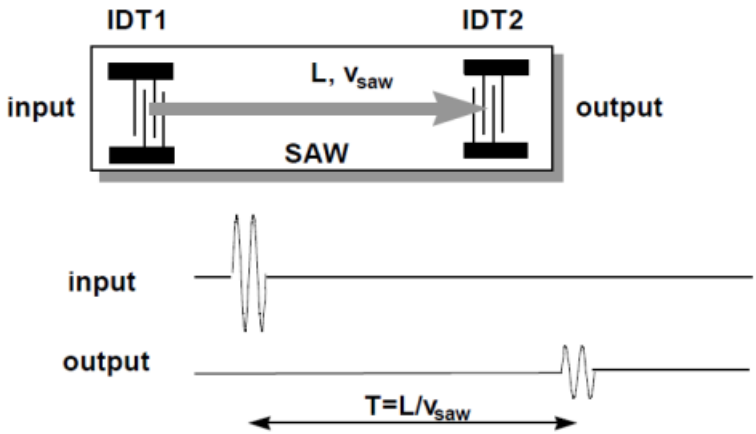

Figure 1.8: Delay line schematic and time response[5]

1.5 One-Port SAW resonator

A one-port resonator consists of one IDT with reflective gratings on either side. The resonant cavity is confined to the region between the reflectors. The waves generated by the IDT produce a standing wave in the resonant cavity which gives the device oscillation frequency. Since SAW devices are inherently small due to their reduced speed in comparison to the electromagnetic wave, these can be used at high frequencies, the highest allowable frequency is limited to the minimum line widths attainable with today's micro-fabrication facilities. For example, in a single-electrode IDT the minimum feature is a:

$$a = \frac{\lambda_{saw}}{4} \iff \lambda_{saw} = \frac{v_{saw}}{f_0} \tag{1.11}$$

$$f_0\Big|_{max} = \frac{v_{saw}}{4 \cdot a|_{min}} \tag{1.12}$$

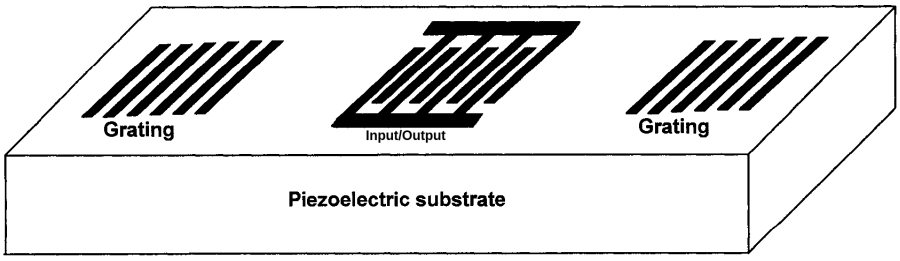

Figure 1.9: One-Port SAW resonator

Quality factor, Q, of a SAW resonator depends on various types of losses in the resonator such as damping loss and energy radiated into the air near the surface of the substrate that can be solved by placing the resonator in an evacuated package. Resonators can be used as frequency control elements in oscillators, as sensors, and as filters in communication systems.
The following parameters must be considered in the design of a SAW One-Port resonator [8]:

1. Number of finger pairs IDTs
2. Acoustic aperture
3. Effective resonant cavity length
4. Number of reflectors in the grating

5. Transducer periodicity
6. Reflector spacing
7. Substrate properties

1.6 Two-Port SAW resonator

A two-port resonator works in the same way as the one-port resonator except there are separate input and output IDTs between the two reflector gratings. Without the reflector gratings, the frequency response will be the same of two IDTs in a cascade, like a delay line SAW device. In the presence of reflector gratings, the frequency response of the resonator around the center frequency will be superimposed on the response of the two IDTs: the response is the same of a delay line except that there is an additional resonant peak at the IDT center frequency.

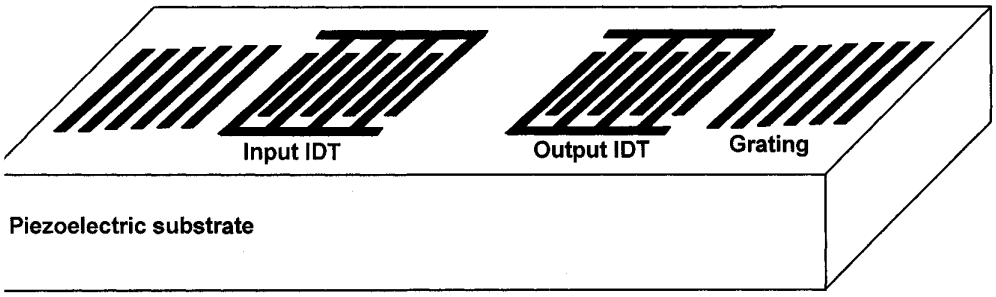

Figure 1.10: Two-Port SAW resonator schematic

The parameters that influence the response of two-port resonator are[8]:

1. Number of finger pairs IDTs
2. Acoustic aperture
3. Separation between grating and the IDTs
4. Separation between IDTs
5. Transducer periodicity
6. Reflector spacing
7. Substrate properties

Chapter 2

Mathematical models

In this chapter, different mathematical models are presented. These are used to predict and optimize the behavior of a SAW device. The first is the "Delta function model" [9]. Through this model, it's possible to obtain only a preliminary transfer function of a SAW device, it doesn't provide any information on input and output impedance or any kind of losses. The others models presented are based on an equivalent circuit model of an IDT: "SAW crossed-field model" which evolves into "Equivalent circuit model"[10][11]. In this way it's possible to consider some of the secondary effects which introduce losses, and influence the harmonic operation of the device. These models give the possibility to treat a SAW device as a transmission line and so use the same rules for electromagnetic waves also for SAW waves.
The final section of this chapter deals with the T-Matrix model[12] that associates a transmission matrix to each element of a SAW device. This model is derived from the Admittance matrix model presented in the section 2.3.The use of matrix blocks simplifies the calculation of the frequency response, since the calculation is limited to the matrix multipliers that compose the system.

2.1 Delta function model

The Delta-Function model provides information about the transfer function of a SAW filter. It cannot provide any information on input and output impedance, circuit factor-loading, harmonic operation, bulk wave interference or diffraction. So, this can only return the relative insertion loss of a SAW filter, but it approximates very well the system behavior of a device using bidirectional IDTs in input and output stages.
In this model the electric field near adjacent electrodes of an IDT is approximated with a discrete number of delta sources. The propagation of surface waves (SAW) in a piezoelectric material may be associated with a surface potential ϕ and electric-field intensity E produced by an excited IDT. The electric field distribution under adjacent electrodes is complex, but, locally, it may be approximated as normal to the piezoelectric surface. This is because the intensity of the electric field distribution is proportional to the instantaneous charge accumulation on adjacent electrodes due to the time-dependent input voltage. At any instant, adjacent electrodes have opposite voltage polarity and opposite charge accumulation. This leads to approximate this charge distribution with a delta source of the electric field at each electrode's edge. So, each electrode is associated with two delta sources and the modulus of the source is related to the intensity of the applied voltage.

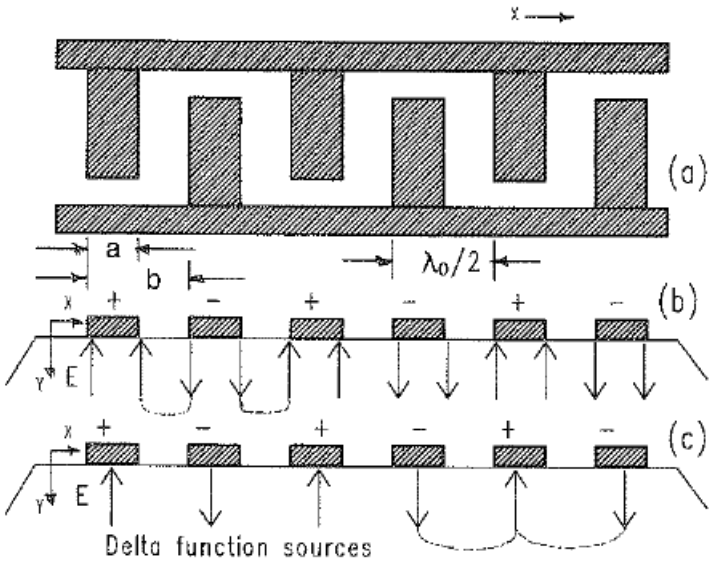

Figure 2.1: Delta function model applied to an IDT[9]

The delta source sign alternates from an electrode to another. The sum of all

contributions coming from each delta source gives the resultant electric field of an excited IDT both at the input and output. The resulting transfer function between input and output can be evaluated extending the calculation to both IDTs.
Another approximation can be done considering a metallization ratio of $\eta = 1$, in this way it is possible to associate with each electrode only a single delta source. This is possible since the delta-function model cannot furnish information on harmonic performance so there isn't a specific reason to consider a different η and consequently use two delta sources for a single electrode. [9].
So, only one delta function is associated for each electrode.

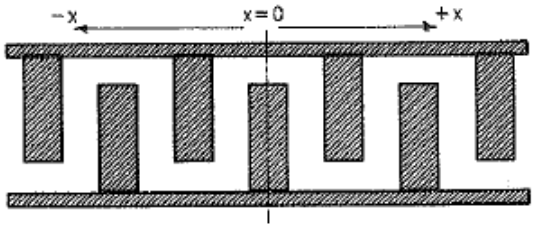

Figure 2.2: Definition of the reference plane to apply the delta function model[9]

Let consider the center in the middle of the IDT, the electric field unitary and assume that N (number of electrodes contained in an IDT is odd, the same consideration will be valid for the even case).
The phase term depends on the distance of the generic point x from each delta source, and this can be expressed as $e^{j\beta x_n}$ with $-x_N \leq x_n \leq x_N$. Then the system frequency response can be written as

$$H_1(f) = \sum_{n=-(N-1)/2}^{(N-1)/2} (-1)^n A_n e^{j\beta x_n} \tag{2.1}$$

Where the value $(-1)^n$, as previously said, represents the alternate polarity of the electric field, the term A_n represents the overlapping region between two electrodes.

$$H_1(f) = \sum_{n=-(N-1)/2}^{(N-1)/2} (-1)^n A_n [\cos \beta x_n - j \sin \beta x_n] \tag{2.2}$$

Choosing the reference axis x=0 in the center of the IDT, the summation results in a simplification of the all sine components in the expression ($\cos(\theta) = \cos(-\theta)$ and $\sin(-\theta) = -\sin(\theta)$). Fixing A_n to 1 and using one delta approximation per

IDT, this means that every electrode is represented by one delta function in the center, every delta is distant from another of the quantity $\lambda_0/2$.

$$H_1(f) = A_n \sum_{n=-(N-1)/2}^{(N-1)/2} (-1)^n \cos \beta x_n \tag{2.3}$$

The transfer function expression can be approximated with a $sinc(x)$ (*the derivation of the following relationship can be found in Appendix A*):

$$X = N_p \pi \cdot \frac{f - f0}{f_0} \tag{2.4}$$

$$|H_1(f)| \propto \left| \frac{\sin X}{X} \right| = \left| \frac{\sin N_p \pi \cdot \frac{f-f0}{f_0}}{N_p \pi \cdot \frac{f-f0}{f_0}} \right| \tag{2.5}$$

The first null occurs when

$$\sin X = 0 \rightarrow X = \pi$$

$$N_p \pi \cdot \frac{f - f_0}{f_0} = \pi$$

$$N_p = \frac{f_0}{f - f_0} = \frac{2}{BW_{nn}} \tag{2.6}$$

BW_{nn} represents the fractional bandwidth which is the first null respect to the central frequency f_0. The fractional bandwidth at $-4dB$ from the main lobe can be approximated to [9]:

$$BW_4 \approx \frac{BW_{nn}}{2} = \frac{1}{N_p} \tag{2.7}$$

Below is reported an example of a frequency response diagram of an IDT with 20 finger pairs, obtained with the delta function model.

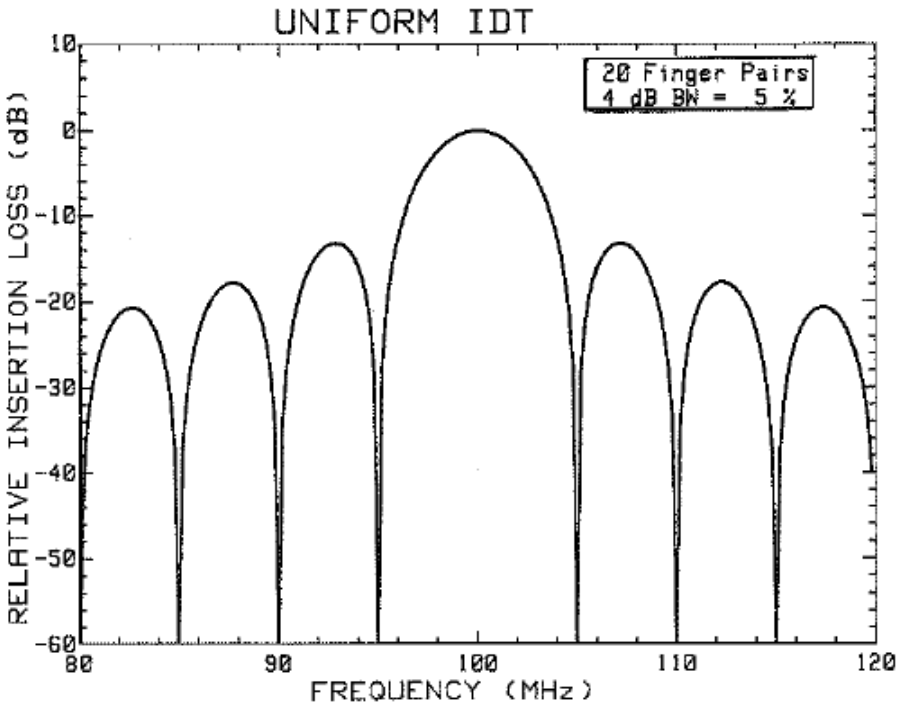

Figure 2.3: The frequency response of an IDT obtained with the delta function model[9]

2.2 SAW crossed-field model

In this model each IDT is represented by a three-port network with 2 acoustic ports and 1 electric port.

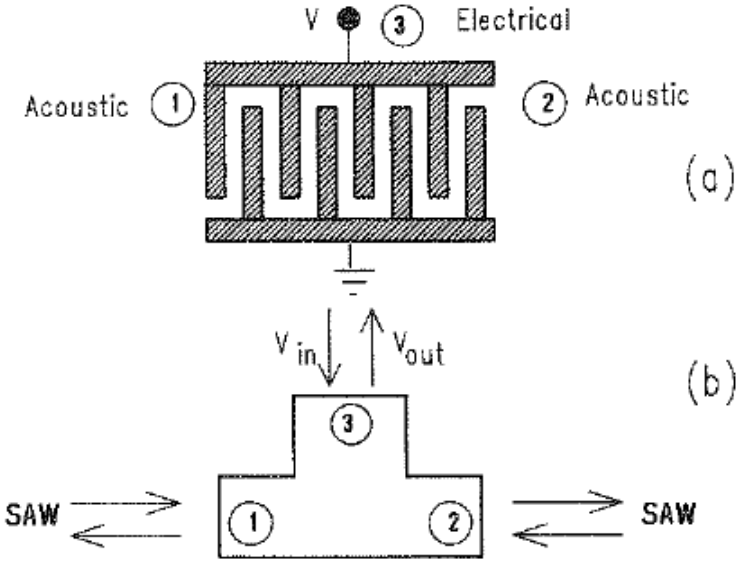

Figure 2.4: (a) Representation of a SAW IDT as a three-port network, Port 1 and 2 are "acoustic" ports while Port 3 is the electrical one. (b) In the crossed-field model Port 1 and 2 are converted into an equivalent electrical transmission line[9]

The following derivations applied to an IDT are neglecting SAW reflections due to IDT finger discontinuities. This approximation leads to set the thickness ratio ($h/\lambda \ll 1\%$) so the radiation conductance $G_a(f)$ parameter will have a sinc-function (symmetric) amplitude response around the center frequency.
For the application of this model, the two acoustic ports (Port1 and Port2) must be converted to electric equivalents; at these ports, acoustic forces F are transformed to equivalent voltages V, while mechanical SAW velocities v are converted to equivalent currents I.

$$V = \frac{F}{\phi} \tag{2.8}$$

$$I = v\phi \tag{2.9}$$

Where ϕ is interpreted as the turn-ratio of an equivalent acoustic-to-electric transformer as sketched in the following picture coming from the *Mason's equivalent model*:

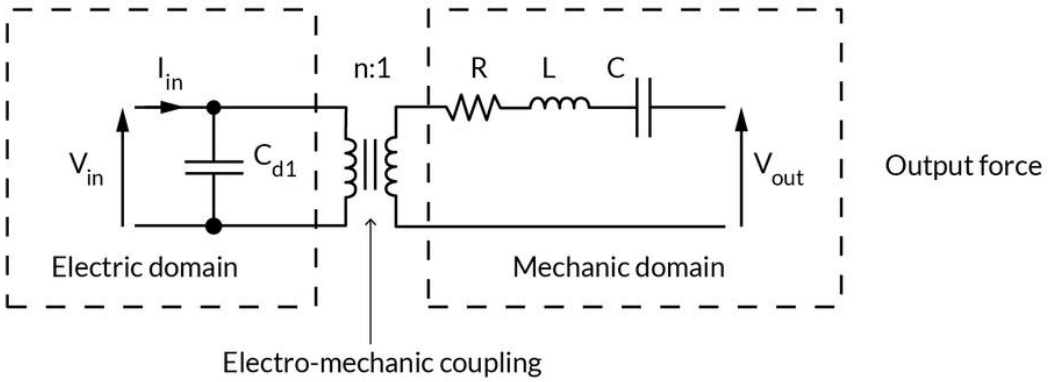

Figure 2.5: Mason's equivalent circuit model

Defining the mechanical characteristic impedance Z_m of the piezoelectric substrate, it is possible to get an equivalent SAW transmission line with characteristic impedance Z_o: for a uniform acoustic wave propagating through a substrate of density $rho(kg/m^3)$ and a large cross-section $A(m^2)$ the mechanical impedance may be written as follows:[10].

$$Z_m = \frac{F}{v} = \rho v A \left[\frac{\text{kg}}{\text{s}}\right] \tag{2.10}$$

where the equivalent electric characteristic impedance can be evaluated as:

$$Z_o = \frac{V}{I} = \frac{F}{v} \cdot \frac{1}{\phi^2} = \frac{Z_m}{\phi^2}[\Omega] \tag{2.11}$$

The equivalent characteristic admittance G_o can be expressed as:

$$G_o = \frac{1}{Z_o} = K^2 C_s f_0 [S] \tag{2.12}$$

Where K^2 is the electromechanical coupling constant, f_0 is the IDT center frequency and $C_s = C_o W$ is the static capacitance of one periodic section. C_o is the capacitance for a finger pair unit [pF/cm] and W is the finger apodization overlap [cm].Once defined the characteristic admittance it's possible to define the three-port admittance matrix [Y] for an IDT:

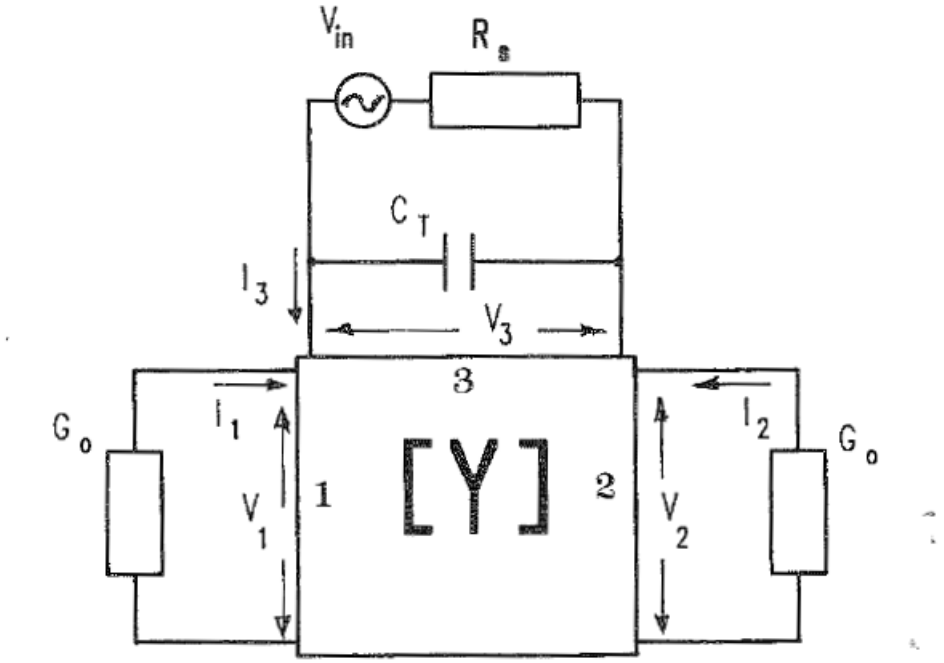

Figure 2.6: Admittance equivalent circuit model[10]

The equivalent matrix expression:

$$[I] = \begin{bmatrix} Y_{11} & Y_{12} & Y_{13} \\ Y_{21} & Y_{22} & Y_{23} \\ Y_{31} & Y_{32} & Y_{33} \end{bmatrix} \cdot [V]$$

The subset of matrix elements $Y_{11}, Y_{12}, Y_{21}, Y_{22}$ represents the equivalent SAW transmission line. For these elements, it can be assumed that they are symmetrical and reciprocal, so

$$Y_{11} = Y_{22} \;\; \& \;\; Y_{12} = Y_{21} \tag{2.13}$$

The terms $Y_{13}, Y_{23}, Y_{31}, Y_{32}$ are related to the acoustic-electric conversion. Thus, it

may be assumed:

$$Y_{13} = Y_{31} \;\; \& \;\; Y_{23} = Y_{32} \tag{2.14}$$

Another assumption can be made by observing that the wave generated at port 2 propagates in the opposite direction of the one generated at port 1, so

$$Y_{13} = -Y_{23} \tag{2.15}$$

The final matrix will assume the form:

$$[Y] = \begin{bmatrix} Y_{11} & Y_{12} & Y_{13} \\ Y_{12} & Y_{11} & -Y_{13} \\ Y_{13} & -Y_{13} & Y_{33} \end{bmatrix} \tag{2.16}$$

These matrix elements for the crossed-field model may be derived to be [10]:

$$Y_{11} = -jG_0 \cot\left(N_p\theta\right) \tag{2.17}$$

$$Y_{12} = jG_0 \csc\left(N_p\theta\right) \tag{2.18}$$

$$Y_{13} = jG_0 \tan\left(\frac{\theta}{4}\right) \tag{2.19}$$

$$Y_{33} = j\omega C_T + j4N_pG_0 \tan\left(\frac{\theta}{4}\right) \tag{2.20}$$

Where $\theta = f/f_0$ and $C_T = N_p \cdot C_0 \cdot W$

The matrix elements explode to infinity at the center frequency because $\theta = 2\pi$, obviously they remain finite, so their values may be calculated by expanding the matrix for frequencies near to the f_0. Calculation of Y_{33} at center frequency

$$Y_{33}(f_0) = \left.\frac{I_3}{V_3}\right|_{f_0} = G_a(f_0) + j2\pi f_0 C_T \tag{2.21}$$

Where $G_a(f_0)$ is the radiation conductance at center frequency such that:

$$G_a(f_0) = 8K^2 f_0 C_S N^2 = 8NG_0 \tag{2.22}$$

Neglecting finger reflections, for frequencies near to the center one the radiation conductance may be approximated with:

$$G_a(f) \approx G_a(f_0) \cdot \left| \frac{\sin X}{X} \right| \tag{2.23}$$

So, the input admittance may also be generalized:

$$Y_{33}(f) = G_a(f) + 2j\pi f C_T \tag{2.24}$$

The equivalent circuit input impedance is sketched below. The same principle can be applied to model the output IDT. In this case, the equivalent excitation source for output IDT is a current.

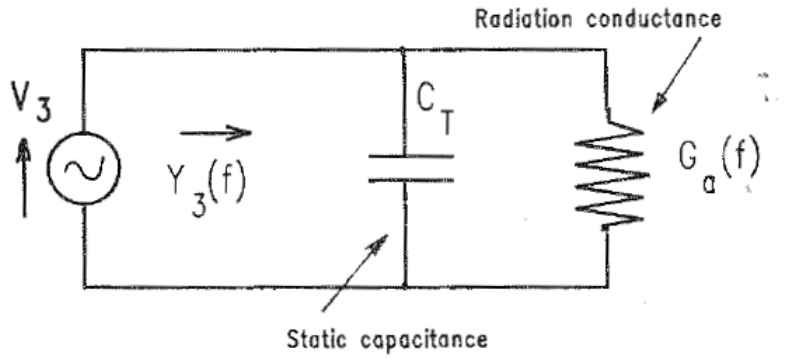

Figure 2.7: Crossed-field equivalent admittance at electrical Port 3, for an IDT at center frequency. Conductance $G_a(f)$ relates power generation from an excited IDT. (Analogous to radiation resistance in an electromagnetic antenna) C_T is the total static capacitance of IDT.[10]

A complete model schematic of an IDT

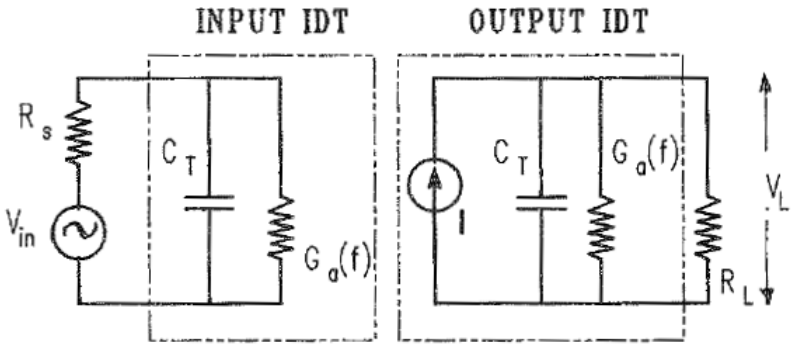

Figure 2.8: Complete model for a SAW device[10]

2.3 Equivalent circuit model

The lumped equivalent circuit model for one IDT finger-section presented below is directly derived from the crossed-field model. The illustration gives a lumped equivalent referred to a metallization ratio $\eta = 0.5$. It incorporates different characteristic impedances for metalized and non-metalized regions of one IDT over a distance of $\lambda_0/2$. The acoustic velocity changes under metallization, reduces with increasing the ratio h/λ_0. The transformer polarities will be dictated by the excitation polarity of the electrode. This transformer ratio is a function of both acoustic aperture and the electromechanical coupling coefficient K^2 of the piezoelectric substrate. This model keeps also trace of electrode discontinuities as susceptance parallel-connected to the electrode, this considers the energy storage at discontinuities. [11]

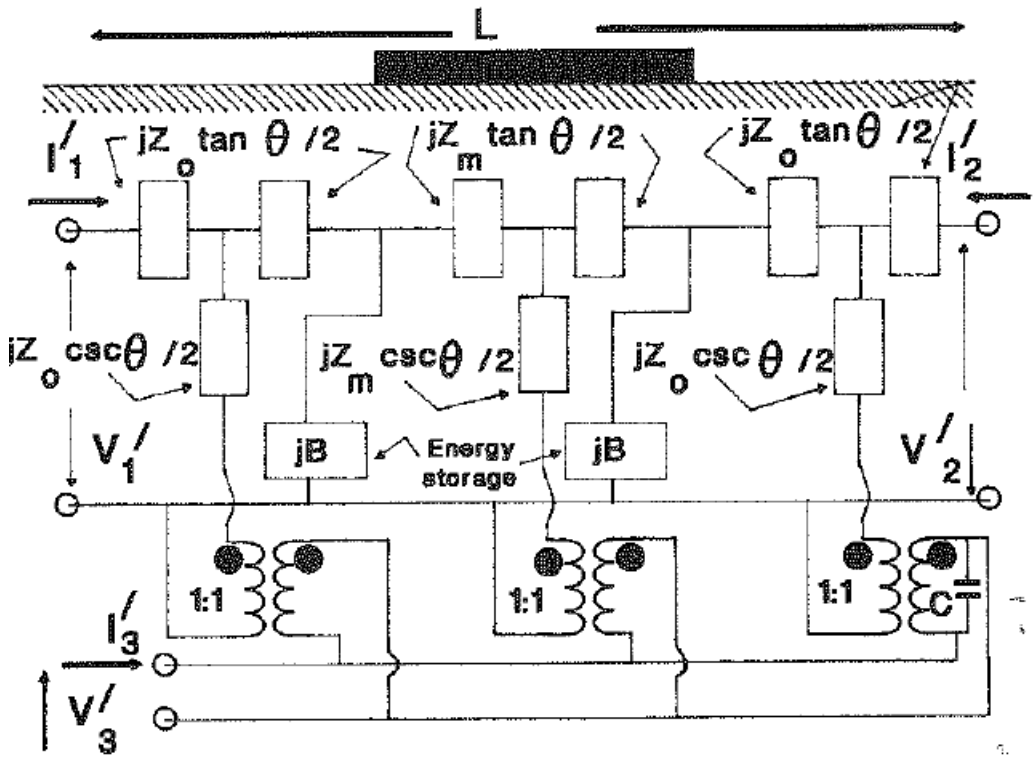

Figure 2.9: Generalized electrical model for an IDT finger[11]

This generalized circuit is able to accurately characterize an IDT, both in fundamental mode and in harmonic mode. In this way, the modeling of an IDT can be applied to solid or split electrodes with arbitrary polarity sequences, as well as to

an arbitrary metallization ratio.[11]
It is known that wave reflections from an obstacle are caused by impedance discontinuities. The same situation prevails for SAW reflections from a metallization strip. Thus, both the SAW velocity and transmission line characteristic impedance have differing values in the metalized and non metalized regions. So, referring to the circuit (Figure 2.9) it is necessary to consider three transmission line equivalent circuits for each section.
The SAW velocity under a metalized region v_m of a single electrode will be reduced by the metal overlay. This implies that characteristic impedance for metalized region is greater than non metalized one.

$$Z_{om} = \frac{1}{G_{om}} > Z_0 \tag{2.25}$$

To obtain the v_m value we need to know the average shifted velocity v_a and the average shifted frequency f_a. The relation between f_a and v_m is given by the following relation:

$$f_a = \frac{1}{2}\left(\frac{\lambda_0}{4v_m} + \frac{\lambda_0}{4v_0}\right)^{-1} \rightarrow f_a = \frac{v_a}{\lambda_0} \tag{2.26}$$

$$v_a = v_0(1 - k_{11})' \tag{2.27}$$

The term v_a is related to the Self-Coupling k_{11} and Mutual-Coupling k_{12} coefficients. The first one considers the effect of the ratio h/λ_0 and it can be expressed in the normalized form as:

$$k'_{11} = \frac{k_{11}}{k_0} = |k'_{11p} + k'_{11m} + k'_{11s}| \tag{2.28}$$

The second one is implemented in the COM analyses of SAW transducers and reflection gratings.

$$k'_{12} = \frac{k_{12}}{k_0} = |k'_{12p} + k'_{12m} + k'_{12s}| \tag{2.29}$$

Here below, there is a table (Table 2.1) that gives values for these parameters related to the specific substrate material used.

Wave Type	Rayleigh	Rayleigh	Rayleigh
Substrate	ST-X Quartz	YZ-LiNbO_3	128^o YX-LiNbO_3
SAW velocity v_o (m/s)	3158	3488	3997
Propagation axis	X	Z	X
Electromechanical coupling coefficient K^2	0.0016	0.045	0.056
C_0 Capacitance finger pair/unit lengh (pF/cm)	0.503	4.5	5.0
k'_{11p}	0.0004	0.018	0.022
k'_{11m}	$0.02(h/\lambda)$	$0.30(h/\lambda)$	$0.091(h/\lambda)$
k'_{11s}	$7.9(h/\lambda)^2$	-	-
k'_{12p}	0.0001	0.0054	0.0064
k'_{12m}	$0.16(h/\lambda)$	$0.08(h/\lambda)$	$0.14(h/\lambda)$
k'_{12s}	-	-	-

Table 2.1: Material parameters table [11]

From the metallization velocity it is possible to derive f_m, the shifted center frequency for the metalized region.

$$f_m = \frac{v_m}{\lambda_0}$$

It is possible to describe each transmission line section of a single IDT finger using ABCD matrix. With the following parameters:

$$\begin{bmatrix} A & B \\ C & D \end{bmatrix} = \begin{bmatrix} \cosh(\gamma d) & Z_o \sinh(\gamma d) \\ \frac{1}{Z_o}\sinh(\gamma d) & \cosh(\gamma d) \end{bmatrix}$$

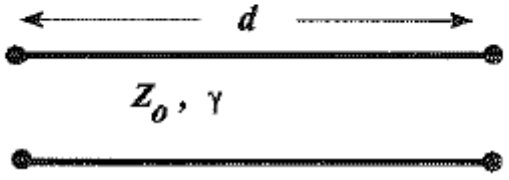

Figure 2.10: ABCD matrix transmission line[11]

The Figure 2.10 recalls the ABCD representation of a transmission line section of

length d, with characteristic impedance Z_0 and propagation constant γ.
The transit angle θ for the non metalized region of characteristic impedance Z_0 and length $d = \lambda_0/8$ is:

$$\theta = \frac{\pi}{4}\frac{f}{f_0} \tag{2.30}$$

The transit angle θ_m of the metalized region of characteristic impedance Z_{0m} and length $d = \lambda_0/4$ is:

$$\theta_m = \frac{\pi}{2}\frac{f}{f_m} \tag{2.31}$$

So, the ABCD matrix for the non metalized region is:

$$[R_u] = \begin{bmatrix} A_u & B_u \\ C_u & D_u \end{bmatrix} = \begin{bmatrix} \cosh j\theta & Z_0 \sinh j\theta \\ \frac{1}{Z_0}\sinh j\theta & \cosh j\theta \end{bmatrix} \tag{2.32}$$

For the metalized region

$$[R_m] = \begin{bmatrix} A_m & B_m \\ C_m & D_m \end{bmatrix} = \begin{bmatrix} \cosh j\theta_m & Z_0 \sinh j\theta_m \\ \frac{1}{Z_0}\sinh j\theta_m & \cosh j\theta_m \end{bmatrix} \tag{2.33}$$

The final ABCD matrix that considers all the three regions is:

$$[R_t] = [R_u][R_m][R_u] \tag{2.34}$$

Now it is possible to extend this result to all fingers in an IDT:

$$[Q] = [R_t]^{2N_p} = \begin{bmatrix} Q_{11} & Q_{12} \\ Q_{21} & Q_{22} \end{bmatrix} \tag{2.35}$$

Where N_p is the finger pairs in the considered IDT. Working backwards, and employing ABCD-to-Y conversion, it is possible to obtain the admittance matrix for the acoustic path:

$$[Y_a^f] = \begin{bmatrix} Q_{22}/Q_{12} & -1/Q_{12} \\ -1/Q_{12} & Q_{11}/Q_{12} \end{bmatrix} \tag{2.36}$$

This result can be incorporated in the 3x3 admittance matrix for an IDT giving the following result:

$$[Y] = \begin{bmatrix} Y_{11}^f & Y_{12}^f & -jG_{0m}\tanh(\alpha + j\theta_m) \\ Y_{21}^f & Y_{22}^f & jG_{0m}\tanh(\alpha + j\theta_m) \\ -jG_{0m}\tanh(\alpha + j\theta_m) & jG_{0m}\tanh(\alpha + j\theta_m) & j\omega C_T + j4N_pG_{0m}\tanh(\alpha + j\theta_m) \end{bmatrix} \tag{2.37}$$

Where α is the attenuation coefficient. The radiation conductance $G_{amf}(f)$ can be obtained with the application of matched boundary conditions such:

$$I_2 = I_1 \rightarrow -\frac{V_1}{Z_0} = -V_1 G_0 = -\frac{V_2}{Z_0} = -V_2 G_0$$

$$G_{amf}(f) = \text{real}\left[\frac{I_3}{V_3}\right] = \text{real}\left[\frac{2Y_{31}^f}{G_0 + Y_{11}^f - Y_{12}^f}\right] \tag{2.38}$$

2.4 Matrix building blocks

This is a more versatile approach that employs the analytical use of transmission matrices. Thanks to this method every element in the SAW resonator schema can be modelled as a "building block" using complex transmission matrices. Building blocks for IDTs are 3x3 transmission matrices relating both acoustic and electric ports. Reflection gratings are 2x2 transmission matrices related only to the acoustic path; also, the space between each building block can be represented as a building block of 2x2 transmission line matrix.
The frequency response of the entire system can be evaluated by multiplying transmission matrices appropriate to each section of the SAW resonator structure and then applying boundary conditions.

2.4.1 Transmission matrix model

In the Transmission matrix model, the building block for the reflection grating $[G]$ is a 2x2 matrix derived from the COM theory [10], that considers an acoustic transmission lines, reflections and losses. The block for the IDT $[T]$, that involves both acoustic and electrical parameters, is a 3x3 matrix derived from the admittance matrix model.
For the free space between building blocks is, also, associated a transmission line acoustic path which in matrix notation is a 2x2 diagonal matrix where the elements represent transmission line segments between two building block components.

Grating Matrix $[G]$

$[G]$ is a 2x2 transmission matrix applied to SAW reflection gratings. For the COM theory is assumed first SAW propagation in a periodic and uniform reflection grating with element spacing period Λ can be represented by a scalar-wave equation as:

$$\frac{\partial^2\phi}{\partial x^2} + \left[\frac{\omega^2}{v^2(x)}\right]\phi = 0$$

ϕ term is quasi-static surface electric potential, ω the angular frequency, and $v(x)$ the SAW velocity; this last term is not constant due to the metallization on the surface, it is perturbed sinusoidally around the value v_0 as the surface wave passes through the gratings. The corresponding Bragg frequency f_0 for the reflection is given by

$$f_0 = \frac{v_0}{2\Lambda} \tag{2.39}$$

Solving the previous equation to first-order for this velocity perturbation, the solution is a pair of coupled-wave equations that describe the "forward" and "backward" SAW propagation. The results in derivative forms are

$$-R' - j\delta R = j\kappa S$$

$$S' - j\delta S = j\kappa R$$

Where R, S (and their derivative) are related to the amplitude of the forward and backward waves, then

$$\delta = \frac{2\pi(f - f_0)}{v_0} + \kappa_{11} \tag{2.40}$$

δ is the frequency deviation from the Bragg frequency f_0 and $\kappa = \kappa_{12}$ is the mutual-coupling coefficient defined before. Using this approach, the grating matrix [G] for a reflection grating is[12]

$$[G] = C\begin{bmatrix} \left[\frac{\sigma}{\kappa} + j\left(\frac{\delta - j\alpha}{\kappa}\right)\tanh\sigma L\right]e^{j\beta_0 L} & je^{j\theta}\tanh(\sigma L)e^{j\beta_0 L} \\ -je^{j\theta}\tanh(\sigma L)e^{-j\beta_0 L} & \left[\frac{\sigma}{\kappa} - j\left(\frac{\delta - j\alpha}{\kappa}\right)\tanh\sigma L\right]e^{-j\beta_0 L} \end{bmatrix} \tag{2.41}$$

$$\sigma = \sqrt{\kappa^2 - (\delta - j\alpha)^2} \tag{2.42}$$

$$C = \left(\frac{\kappa}{\sigma}\right)\cosh\sigma L \tag{2.43}$$

κ is the grating mutual coupling coefficient (m^{-1}), α is the grating attenuation constant (m^{-1}), L is the grating length (m), $\beta_0 = \omega_0/v_0$ is the "unperturbed" phase constant (rad/s). For a narrowband approximation, it is possible to introduce a normalized term of the frequency deviation (eq. 2.48) Δ:

$$\Delta = \frac{\delta}{\kappa} \tag{2.44}$$

So, σ becomes if we consider $\alpha = 0$:

$$\sigma = \sqrt{\kappa^2 - \delta^2} = \lambda\sqrt{1 - \Delta^2} \tag{2.45}$$

During the computation of the frequency response, it is important to correctly identify the reference axes for matrix relationship. As in a transmission line the notation used to identify a progressive wave is "+", for a regressive wave "-".

$$[W_i] = \begin{bmatrix} w_i^+ \\ w_i^- \end{bmatrix}$$

Considering, for example a Reflection Grating the notation becomes

$$[W_{i-1}] = [G][W_i] \tag{2.46}$$

In the picture below it is possible to observe graphically the relation shown above:

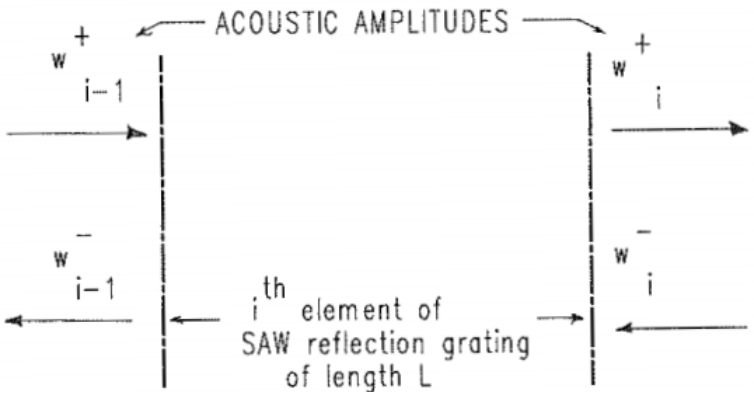

Figure 2.11: The SAW reference planes at i-th element of a SAW reflection grating of length L[12]

From this element, a one-dimensional transmission line type of equation for the electric potential ϕ on the surface of the piezoelectric substrate can be solved as

$$\phi(x) = w^+(x)e^{-j\beta_0 x} + w^-(x)e^{j\beta_0 x}$$

$\beta_0 = \pi/\Lambda$ is the propagation constant of the surface acoustic wave at the Bragg frequency ($f_0 = v_0/2\Lambda$) when the grating has a maximum reflection coefficient. This acoustic wave equation is solved considering the SAW amplitudes at the start x=0 and at the end x=-L. For narrow frequencies around the center frequency f_0:

$$[W(-L)] = [G][W(0)] \tag{2.47}$$

The length L of the grating block, where N_g is the number of reflection elements, is

$$L = N_g \cdot \Lambda \tag{2.48}$$

If there isn't an incident SAW wave at the plane $x = 0$ then at the reference plane $x = -L$ the reflection coefficient at the center frequency is

$$\rho(\Delta = 0) = \frac{w^-(-L)}{w^+(-L)} = \left.\frac{G_{21}}{G_{22}}\right|_{\Delta=0} = j \tanh|\sigma L| \tag{2.49}$$

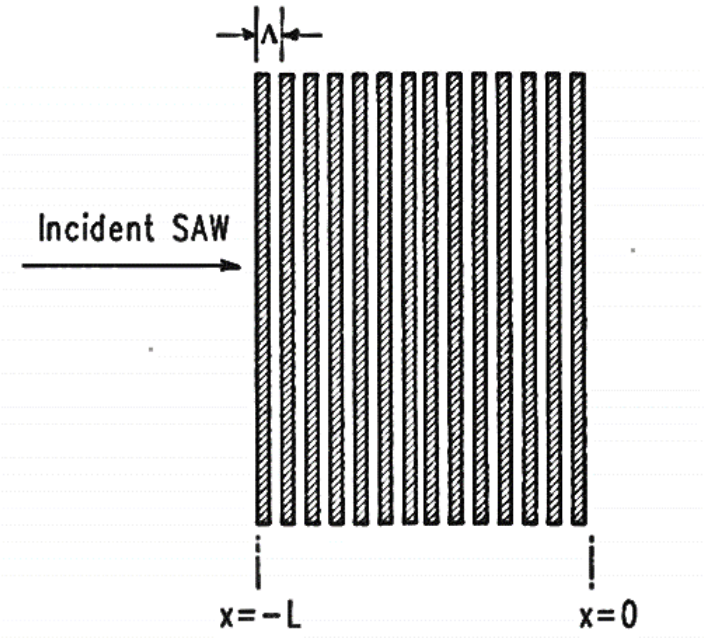

Figure 2.12: Incident SAW on a SAW reflection grating of length L[12]

It is important to notice that the j-term contained in the previous equation is a result of the reference axis chosen, that is $\lambda/8$ away from the physical edge of the first grating element. This shift corresponds to a 90 degree rotation on the Smith Chart. If the reference plane is moved to the leading edge of the first element, the reflection coefficient magnitude as the center frequency is approximated as:

$$\left.\rho\right|_{\Delta=0} = (-1)^n \tanh|\sigma L| \tag{2.50}$$

The index n is chosen to fit experimental reflection data in the following table.

	Sign of Reflection coefficient ρ	Velocity perturbation in strip $\Delta v/v$
YZ-LiNbO_3 (shorted)	$-$	-0.018
YZ-LiNbO_3 (open)	$+$	-0.006 to -0.010

Table 2.2: Measured characteristic of some Rayleigh-wave Reflection grating types, extracted table from Table 11.2 [13]

According to the table 2.2 with lithium niobate n=0 considering open metal strip gratings or n=1 for shorted metal strips.

3x3 IDT matrix

A 3x3 transmission matrix is necessary to link the electrical and acoustic parameters of each IDT. This $[T]$ transmission matrix can be represented by these equations:

$$\begin{bmatrix} w_{i-1}^{+} \\ w_{i-1}^{-} \\ b_i \end{bmatrix} = [T] \begin{bmatrix} w_i^{+} \\ w_i^{-} \\ a_i \end{bmatrix}$$

Where b_i and a_i denote complex electrical tensions at output and input for the i-th port. Reference planes for the IDT are shown in the following figure:

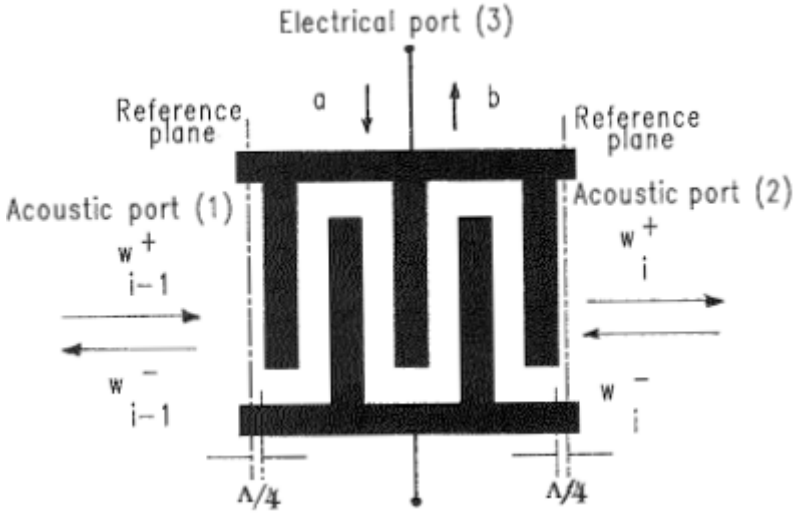

Figure 2.13: Reference planes at offsets $\lambda/8 = \Lambda/4$, as used before for an IDT, together with acoustic and electrical ports.[12]

The IDT matrix elements are given as [12]

$$[T] = \begin{bmatrix} t_{11} & t_{12} & t_{13} \\ -t_{12} & t_{22} & t_{23} \\ st_{13} & -st_{23} & t_{33} \end{bmatrix} \tag{2.51}$$

s is a symmetric parameter and $s = 1$ or $s = -1$ for an IDT with an even or odd number of electrodes N_t.
The systems of equation that describes the relation between electric and acoustic port is the following one:

$$[W_{i-1}] = [t_l][W_i] + a_i[\tau_i] \tag{2.52}$$

$$b_i = [\tau_i'][W_i] + a_i[t_{33}] \tag{2.53}$$

where

$$[t_l] = \begin{bmatrix} t_{11} & t_{12} \\ -t_{12} & t_{22} \end{bmatrix}$$

$$[\tau_i] = \begin{bmatrix} t_{13} \\ t_{23} \end{bmatrix}$$

$$[\tau_i'] = s \begin{bmatrix} t_{13} \\ -t_{23} \end{bmatrix}$$

[T] may be expressed as:

$$[T] = \begin{bmatrix} s(1+t_0)e^{j\theta_t} & -st_0 & t_{13} \\ st_0 & s(1-t_0)e^{j\theta_t} & t_{13}e^{-j\theta_t} \\ st_{13} & -st_{13}e^{-j\theta_t} & t_{33} \end{bmatrix} \tag{2.54}$$

Where every term of the preceding matrix may be expressed as.

$$t_0 = \frac{G_a(R_s + Z_e)}{1 + j\theta_e} \tag{2.55}$$

$$t_{13} = \frac{\sqrt{2G_aZ_e}}{1 + j\theta_e} e^{j\theta_t/2} \tag{2.56}$$

$$t_{33} = 1 - \frac{2j\theta_c}{1 + j\theta_e} \tag{2.57}$$

$$s = (-1)^{N_t} \tag{2.58}$$

The transit angles can be expressed as

$$\theta_t = N_t \Lambda \delta \tag{2.59}$$

$$\theta_c = \omega C_T (R_s + Z_e) \tag{2.60}$$

$$\theta_e = (\omega C_T + B_a)(R_s + Z_e) \tag{2.61}$$

Where C_T is the total IDT capacitance:

$$C_T = \frac{(N_t - 1)C_s}{2}$$

C_s is the static-capacitance per electrode pair, Z_e is the load or source resistance, N_t is the number of IDT electrodes, R_s is the combined IDT metal and lead resistance. The radiation conductance can be expressed, assuming that finger reflection can be neglected, as

$$G_a = G_0(N_t - 1)^2 \left[\sin\frac{\theta_t}{2} / \frac{\theta_t}{2}\right]^2 \iff G_0 = 8K^2 C_s f_0 \tag{2.62}$$

where K^2 is the electromechanical coupling constant; the corresponding radiation susceptance B_a is

$$B_a \approx 2G_0(N_t - 1)^2 \frac{\sin\theta_t - \theta_t}{\theta_t^2} \tag{2.63}$$

Acoustic transmission Line [D]

This matrix represents the acoustic transmission line between two elements in a SAW resonator. The relation that correlates the input SAW wave and the output is the following:

$$[W(d)] = [D][W(0)]$$

where the matrix [D] is

$$[D] = \begin{bmatrix} e^{j\beta d} & 0 \\ 0 & e^{-j\beta d} \end{bmatrix} \iff \beta = \frac{2\pi}{\lambda} \tag{2.64}$$

d is the acoustic length between two blocks.

Chapter 3

Device modelling

In this work, a SAW transponder was implemented as a two-port SAW resonator, in which one port is connected to an antenna and the other to an external sensor. This transponder does not have an ID.
The substrate used for the realization of this device is YZ cut $LiNbO_3$. The working frequency f_0 is chosen according to the resolution of the laser writer machine, used to obtain the mask for the photolithography process. This because the dimensions of the shapes which compose the device are related to the SAW wavelength by the relation:

$$\lambda_{SAW} = \frac{v_{SAW}}{f_0} \tag{3.1}$$

The maximum photolithographic resolution, for the available machine, is about 1 μm, the SAW speed is $3488 m/s$ (Table 2.1) and $\lambda/4$ is the minimum size (for a single finger IDT) so the maximum achievable working frequency of the device is:

$$f_0\Big|_{max} = \frac{3488\text{m/s}}{4 \cdot 1\mu\text{m}} = 872\text{MHz} \tag{3.2}$$

For the current project, the center frequency is 100 MHz. It is below the maximum frequency calculated above and thus belongs to the constraints imposed by the photolithography process. Once the operating frequency has been set, the IDT parameters of the device can be calculated:

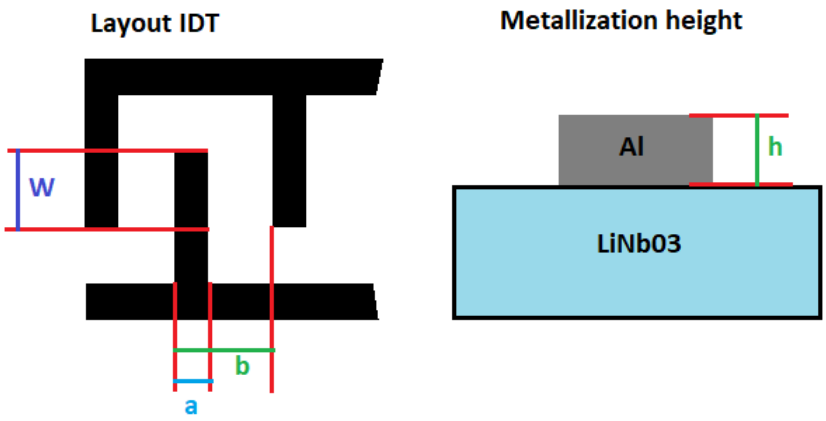

Figure 3.1: Definition of the IDT structure and constitutive parameters

Since $a = \lambda_{SAW}/4$ (single finger) and using a metallization ratio $\eta = a/b = 0.5$:

$$\lambda = \frac{3488\text{m/s}}{100\text{MHz}} = 34.88\mu\text{m} \tag{3.3}$$

$$a = \frac{\lambda}{4} = 8.72\mu\text{m} \tag{3.4}$$

$$b = 2a = 17.44\mu\text{m} \tag{3.5}$$

In order to reduce the finger reflection coefficient, the thickness ratio must be $h/\lambda \ll 1\%$:

$$h \ll 0.01 \cdot \lambda = 348\text{nm} \iff h = 100\text{nm} \tag{3.6}$$

The apodization width is choosen to be $W = 80\lambda = 2.79\text{mm}$. Using the Table 2.1 it is possible to extract the others IDT parameters. The static capacitance for an IDT finger pair:

$$C_s = C_0 \cdot W = 4.5\text{pF/cm} \cdot 80\lambda = 1.25\text{pF/pair} \tag{3.7}$$

The characteristic admittance for the SAW transmission line:

$$G_0 = K^2 C_s f_0 = 0.045 \cdot 1.25\text{pF} \cdot 100\text{MHz} = 5.65\mu\text{S} \tag{3.8}$$

Self-Coupling k_{11} and Mutual-Coupling k_{12} coefficients

$$k'_{11} = |k'_{11p} + k'_{11m} + k'_{11s}| = 0.018 + 0.30 \cdot \frac{h}{\lambda} = 0.0188 \tag{3.9}$$

$$k'_{12} = |k'_{12p} + k'_{12m} + k'_{12s}| = 0.0054 + 0.08 \cdot \frac{h}{\lambda} = 0.0056 \tag{3.10}$$

To simulate the device response, the T-matrix model was implemented. Using relationships shown in the previous chapter, section (2.4.1), it is possible to obtain the equivalent transmission matrix for an IDT, and reflection grating elements. Figure 3.2 shows the layout of the two-port resonator used to make the SAW transponder.

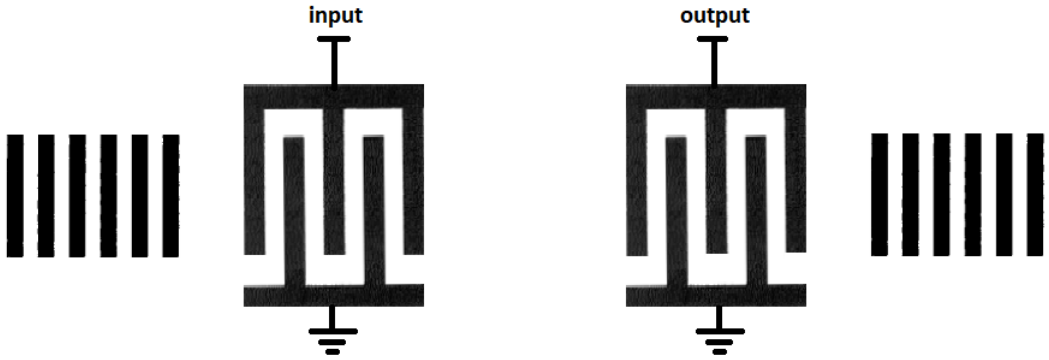

Figure 3.2: Layout of the generic Two-Port SAW resonator

Each element in the Figure 3.2 can be converted in a basic block and concatenated with the others as shown in the Figure 3.3.

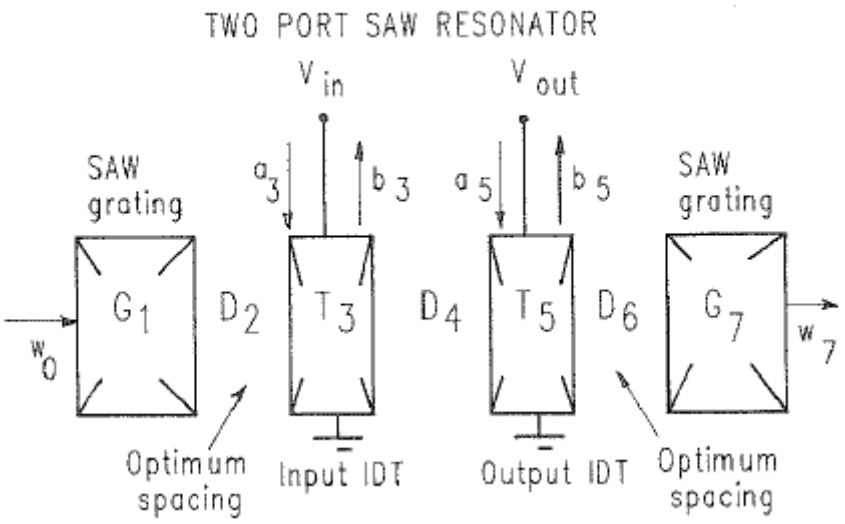

Figure 3.3: Device block schematic[12]

Each element can be associated with a specific transmission matrix characterized by the following relations:

- for an IDT block:
$$\begin{bmatrix} W_{i-1}^{+} \\ W_{i-1}^{-} \\ b_i \end{bmatrix} = \begin{bmatrix} T & B \\ C & t_{33} \end{bmatrix} \begin{bmatrix} W_i^{+} \\ W_i^{-} \\ a_i \end{bmatrix}$$

- for a grating block:
$$\begin{bmatrix} W_{i-1}^{+} \\ W_{i-1}^{-} \end{bmatrix} = \begin{bmatrix} G \end{bmatrix} \begin{bmatrix} W_i^{+} \\ W_i^{-} \end{bmatrix}$$

- for a Spacing block:
$$\begin{bmatrix} W_{i-1}^{+} \\ W_{i-1}^{-} \end{bmatrix} = \begin{bmatrix} D \end{bmatrix} \begin{bmatrix} W_i^{+} \\ W_i^{-} \end{bmatrix}$$

Where W_{I-1}^{+} and W_{I-1}^{-} represent, respectively the incident and the outgoing SAW from the left side of the block, meanwhile W_I^{+} and W_I^{-} are respectively the outgoing wave and the incident wave from the right side. a and b are the incident and reflected electromagnetic wave at the IDT electrical port.
Using the block diagram shown in Figure 3.3 it is possible to solve the system of equations and obtain the frequency response of the device. Thanks to the

modularity of each element, a block can be combined with adjacent ones to obtain a unique relationship between input and output

$$\begin{bmatrix} W_0^+ \\ W_0^- \end{bmatrix} = \begin{bmatrix} G_1 \end{bmatrix} \begin{bmatrix} W_1^+ \\ W_1^- \end{bmatrix} \tag{3.11}$$

$$\begin{bmatrix} W_1^+ \\ W_1^- \end{bmatrix} = \begin{bmatrix} D_2 \end{bmatrix} \begin{bmatrix} W_2^+ \\ W_2^- \end{bmatrix} \tag{3.12}$$

by substituting $\begin{bmatrix} W_1^+ \\ W_1^- \end{bmatrix}$ (eq. 3.12) in the first equation (eq. 3.11):

$$\begin{bmatrix} W_0^+ \\ W_0^- \end{bmatrix} = \begin{bmatrix} G_1 \end{bmatrix} \begin{bmatrix} D_2 \end{bmatrix} \begin{bmatrix} W_2^+ \\ W_2^- \end{bmatrix} \tag{3.13}$$

Repeating this process for all blocks in the schema (Figure 3.3):

$$\begin{bmatrix} W_0^+ \\ W_0^- \end{bmatrix} = [G_1][D_2][T_3][D_4][T_5][D_6][G_7] \begin{bmatrix} W_7^+ \\ W_7^- \end{bmatrix} + [G_1][D_2][B_3]a_3 + \\ + [G_1][D_2][T_3][D_4][B_5]a_5 \tag{3.14}$$

$$b_3 = [C_3][D_4][T_5][D_6][G_7] \begin{bmatrix} W_7^+ \\ W_7^- \end{bmatrix} + (t_{33})_3 a_3 + [C_3][D_4][B_5]a_5 \tag{3.15}$$

$$b_5 = [C_5][D_6][G_7] \begin{bmatrix} W_7^+ \\ W_7^- \end{bmatrix} + (t_{33})_5 a_5 \tag{3.16}$$

These relations can be compressed by substituting these long product terms with:

$$\begin{bmatrix} W_0^+ \\ W_0^- \end{bmatrix} = [M] \begin{bmatrix} W_7^+ \\ W_7^- \end{bmatrix} + [N]a_3 + [K]a_5 \tag{3.17}$$

$$b_3 = [L] \begin{bmatrix} W_7^+ \\ W_7^- \end{bmatrix} + (t_{33})_3 a_3 + [P]a_5 \tag{3.18}$$

$$b_5 = [R] \begin{bmatrix} W_7^+ \\ W_7^- \end{bmatrix} + (t_{33})_5 a_5 \tag{3.19}$$

Applying the boundary conditions in which is considered, there are no incoming SAW waves from external boundaries of the device and there isn't an input voltage on the output port. So

$$W_0^+ = W_7^- = 0 \text{ and } a_5 = 0$$

The previous equations become:

$$\begin{bmatrix} 0 \\ W_0^- \end{bmatrix} = [M] \begin{bmatrix} W_7^+ \\ 0 \end{bmatrix} + [N]a_3 + 0 \tag{3.20}$$

$$b_3 = [L] \begin{bmatrix} W_7^+ \\ 0 \end{bmatrix} + (t_{33})_3 a_3 + 0 \tag{3.21}$$

$$b_5 = [R] \begin{bmatrix} W_7^+ \\ 0 \end{bmatrix} + 0 \tag{3.22}$$

A MATLAB program, which implements the equations 3.20,3.21,3.22, has been developed to simulate the device behaviour. The code is shown in the appendix B. Here below are reported the results obtained from the five different devices realized and a table which summarizes the differences between each.

Device no.	Input finger pairs IDT	Output finger pairs IDT
1	8	8
2	15	8
3	15	15
4	40	15
5	50	15

Table 3.1: Summary of devices

The following graphs represent the transmission coefficient S_{21} of each device in dB. This value shows the device's ability to transmit a signal from input to output, in other words how much a signal at a certain frequency is attenuated by the device.

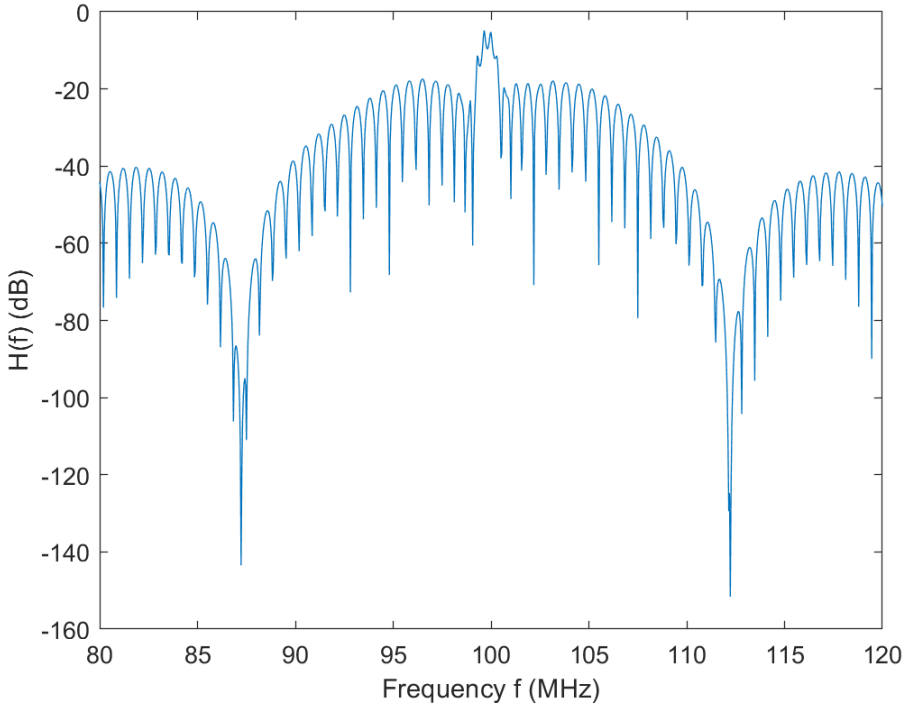

Figure 3.4: Input/Output relations 8 finger pairs at input 8 finger pairs at output

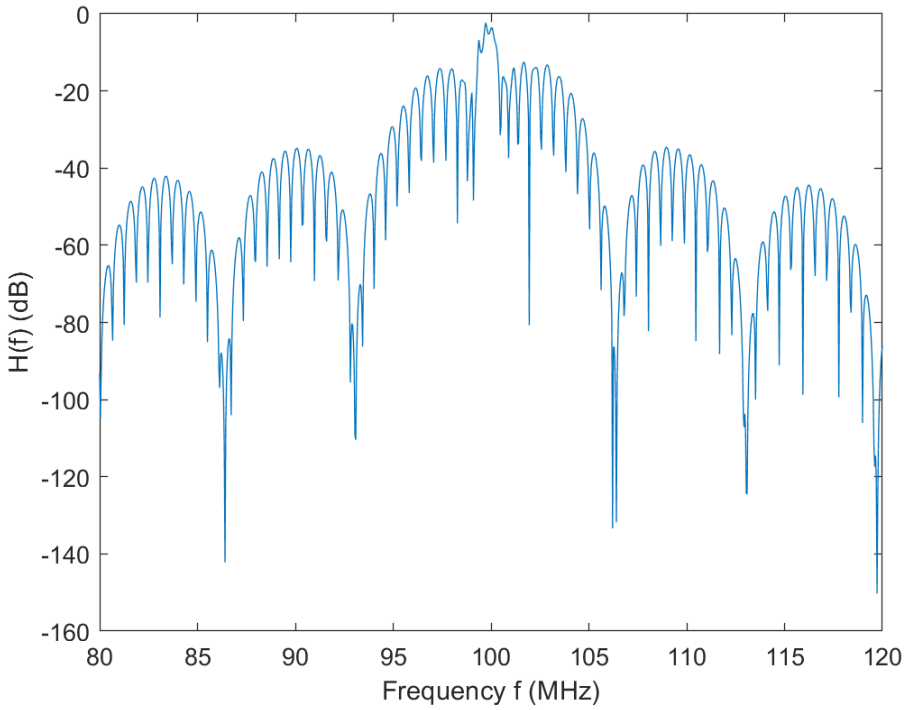

Figure 3.5: Input/Output relations 15 finger pairs at input 15 finger pairs at output

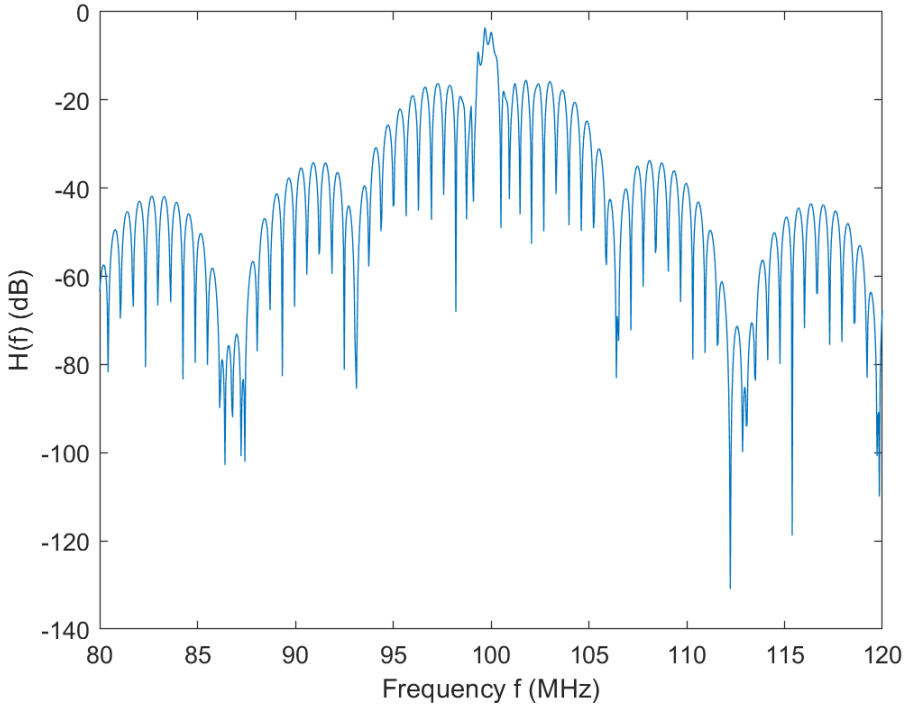

Figure 3.6: Input/Output relations 15 finger pairs at input 8 finger pairs at output

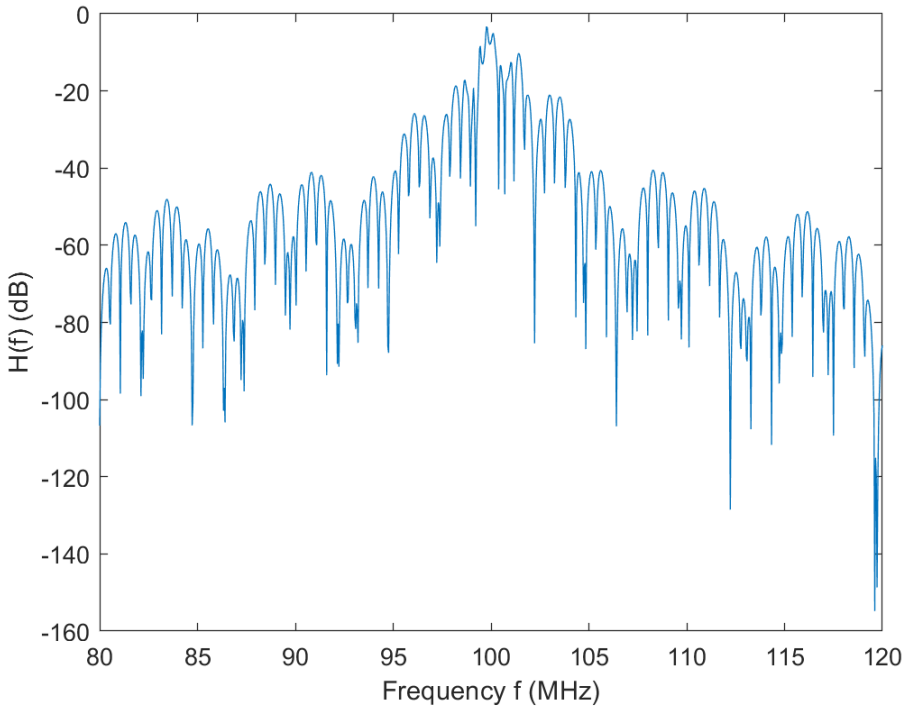

Figure 3.7: Input/Output relations 40 finger pairs at input 15 finger pairs at output

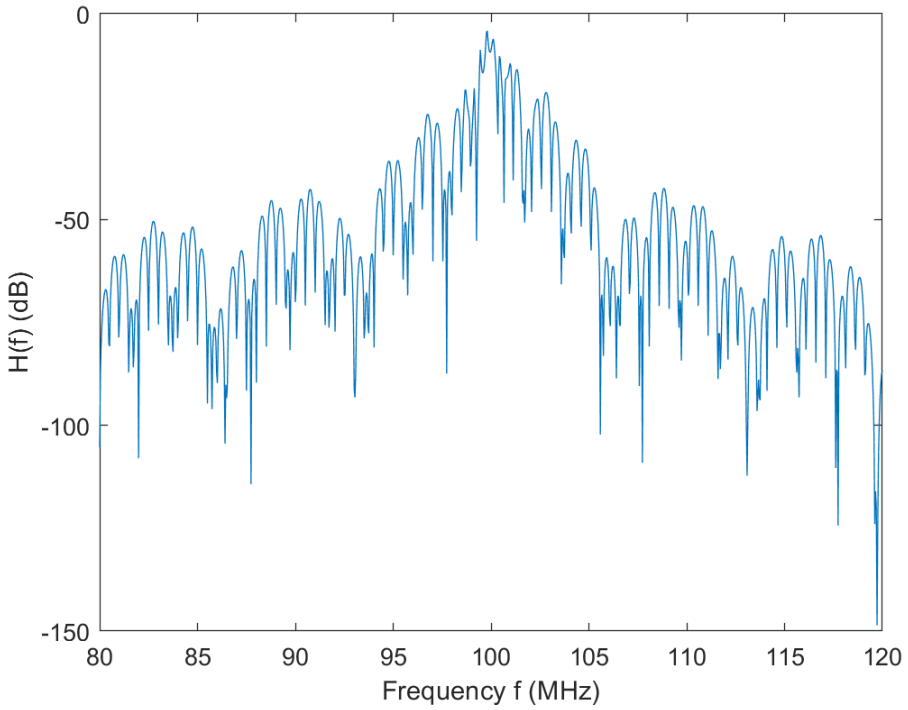

Figure 3.8: Input/Output relations 50 finger pairs at input 15 finger pairs at output

From these graphs it is possible to observe that around the working frequency (100MHz) the transmission coefficient S_{21} reduces the signal attenuation (it goes from about -20 dB to the interval between -10 dB and 0 dB). It is possible, also, to observe clearly in the figures (3.4, 3.5, 3.6) the SAW delay line frequency response with the superimposed resonant peak of the resonator at the center frequency which causes the reduction of the attenuation around that frequency. Later these charts will be compared with the ones obtained by the real devices.

Chapter 4

Device Realization

In this preliminary design phase, five different devices were manufactured to obtain a SAW transponder to assess which is best for this purpose. These differ from each other for a different number of finger pairs of input and output IDTs. Below is reported the Table 3.1:

Device no.	Input finger pairs IDT	Output finger pairs IDT
1	8	8
2	15	8
3	15	15
4	40	15
5	50	15

Table 4.1: Summary of devices

The *CleWin 5.2 Layout Editor* program was used to make the mask layout, and for this purpose a python program was developed to realize each single element of the mask. Thanks to this program, the creation and modification of each element were faster and more precise; the program interface is illustrated below and the code is attached in the appendix.

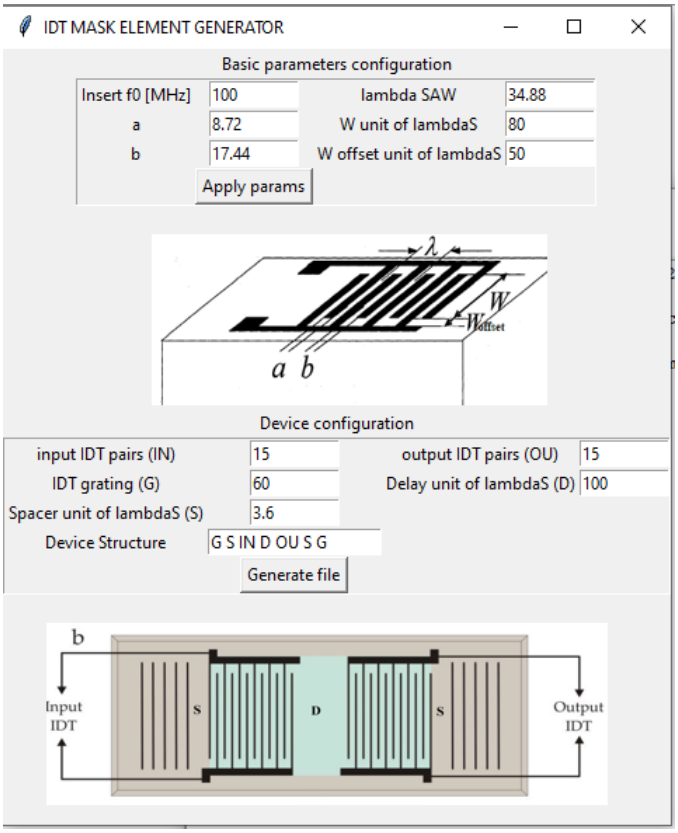

Figure 4.1: "IDT MASK ELEMENT GENERATOR" program. Through this interface, it is possible to generate a SAW device by setting the working frequency, the number of finger pairs in input and output, etc.... It is also possible to set the sequence order of the elements in the "Device structure" field

The program output is a * .cif file that can be opened and edited with *CleWin 5.2 Layout Editor*. After the creation of each single device, these were grouped to make the mask as shown in Figure 4.2. The devices have been positioned to maximize the occupied area and reduce the waste of material.

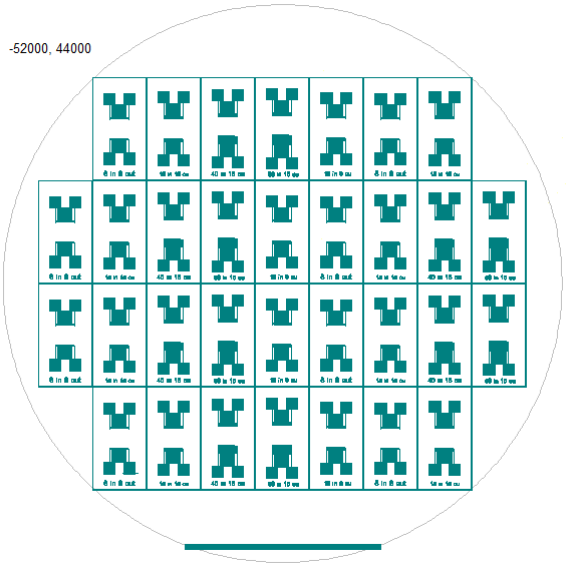

Figure 4.2: MASK layout, with the horizontal flat band for the mask alignment

The mask was made using a chrome-coated 5-inch square quartz glass and a negative resist, so to get the desired design on the mask (Figure 4.2) it was necessary to make the negative of the previous image:

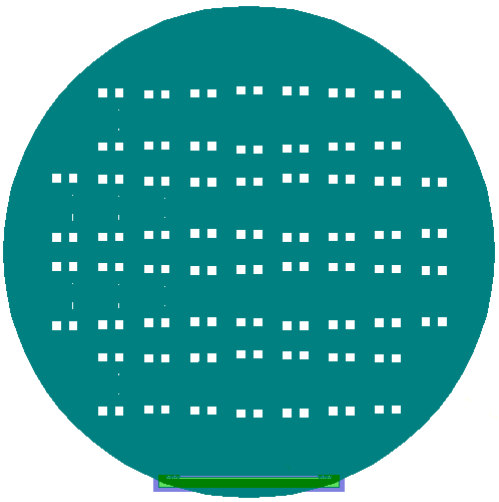

Figure 4.3: Negative MASK layout

The resist on the mask was exposed in the laser writing machine

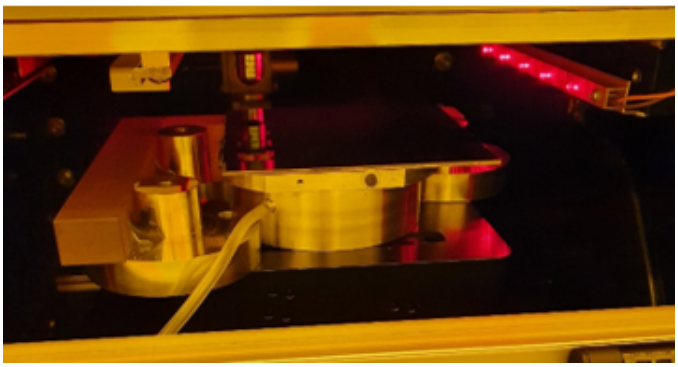

Figure 4.4: Laser writer: writing on the mask

The writing procedure lasted about 11 hours. The mask developing process consist of the removing the resist, chrome and anti-reflecting coating on the exposed parts of the mask. This step requires only a few minutes. The resist development consists in immersing the mask for about 30 seconds in a 1:3 diluted solution of AZ400K Developer and distilled water. After several flushing with clean water, the resist in the exposed areas is removed. Using the Chrome Etchant (UN1760) the exposed chrome is removed from the mask. Figure 4.5 shows the result of this process.

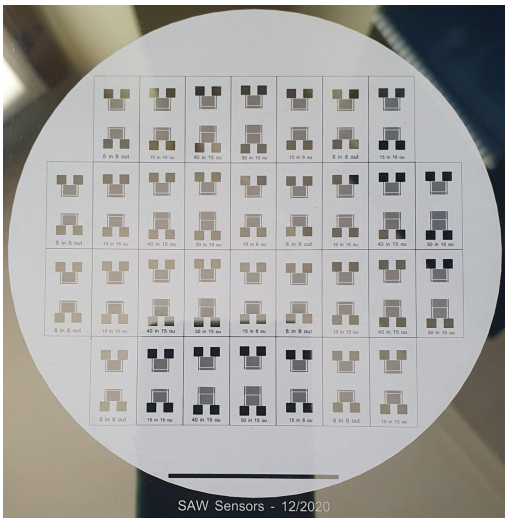

Figure 4.5: Mask after chrome etching, on the bottom is present the flat band to align the mask and wafer during the exposure process

The devices are obtained using the Lift-Off process. This consists of making a negative pattern on the wafer surface of all devices, the unexposed areas of the resist can be dissolved in a developing solution leaving voids. These can be filled with metal or other materials. Then another solvent is used to remove the remaining resist in order to peel off the excess material on the surface. The process steps are summarized below:

- Making negative resist film on the wafer surface: spinning and baking process.
- Resists exposure (surface pattern): UV exposure and soft bake.
- Resist development (removal of unexposed resist)
- Verification of the resulting patterns under the microscope.
- Metal deposition: Al deposition by high vacuum evaporator.
- Lifting Process: Remove residual resist to detach the excess metal.
- Verification of the resulting patterns under the microscope.

The first step is to prepare the $LiNbO_3$ wafer for the UV development process. The wafer is posed in the machine for spinning procedure: a diluted (2:1) NLOF negative resist solution is deposited on the material surface and rotated at 3000 rpm for 60 seconds, this allows to realize a covering film with a thickness of about 1 μm. To dry the resist a soft bake is applied for 2 minutes at 100°C.

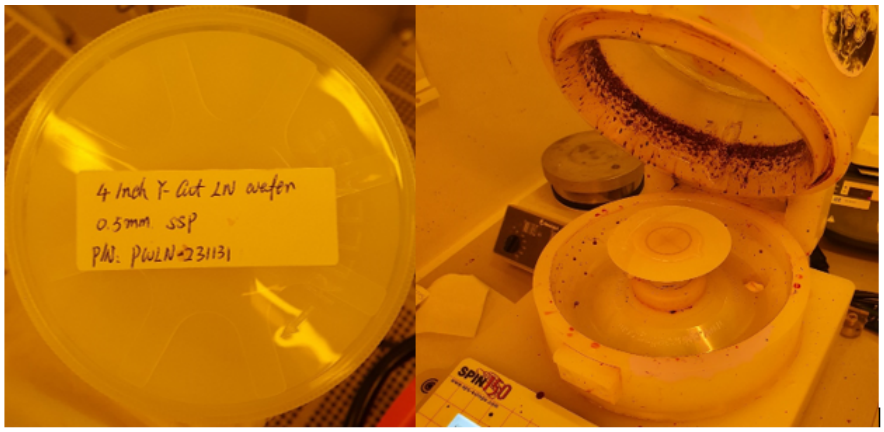

Figure 4.6: Spinning process

Then both the mask and wafer are placed in the UV exposure, the wafer flat band has been aligned with the horizontal flat on the mask, then starts the exposure

for 16 seconds at 16 mW of power to the UV light. To finalize the image transfer process a 1 minute post exposure bake is done (always 100°C).

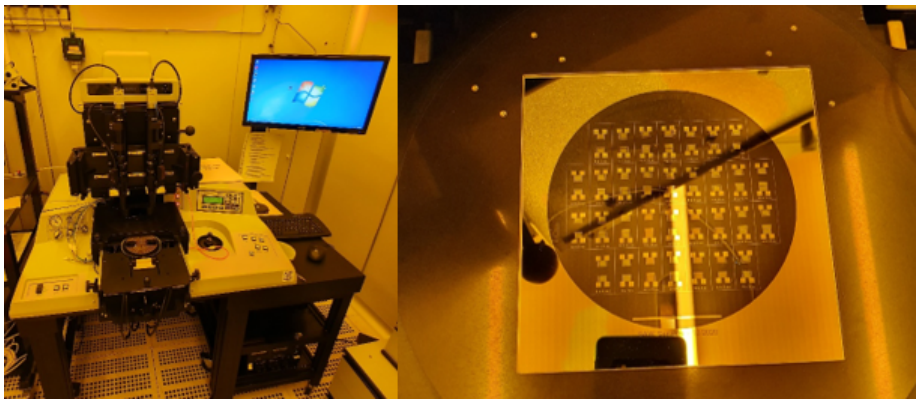

Figure 4.7: UV exposure machine on the left, and mask positioning on the right

This process was repeated 3 times to obtain acceptable characteristics of the devices. Due to the thickness of the resist, after the wafer development process the IDT structures collapsed making the devices unusable. To solve this, the exposure time was changed to 16 seconds.

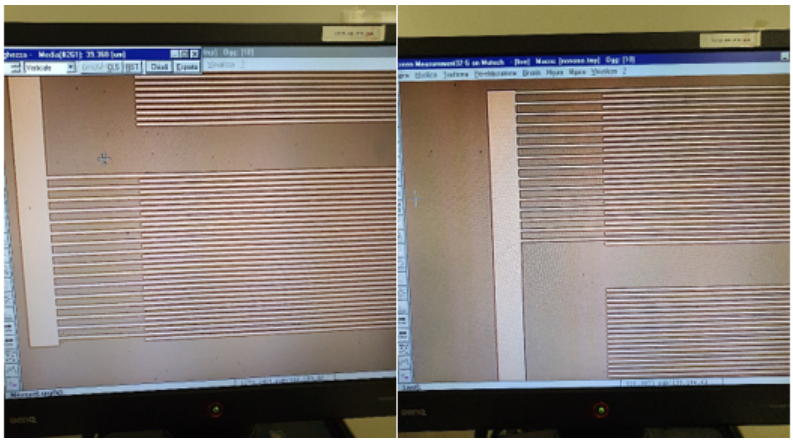

Figure 4.8: Device checking features

Once the expected result has been obtained, it is possible to proceed with the deposition of the aluminum on the surface, the thickness of the Al is 100 nm (eq. 3.6). A high vacuum evaporator is required for this process ($0.55 \cdot 10^{-6}$ bar). Evaporation takes place via a high-energy electron beam focused for a few seconds in a melting pot containing aluminum.

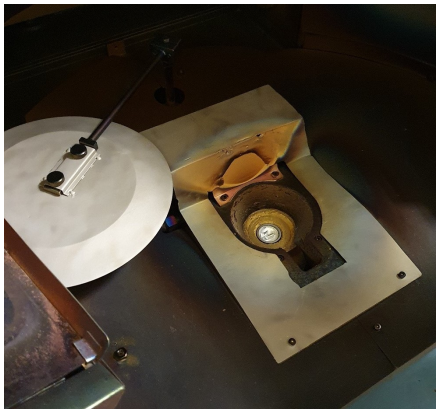

Figure 4.9: Evaporation chamber with melting pot containing aluminum

Figure 4.10: High Vacuum Evaporator

The wafer is fixed on a rotating support as shown in the picture below

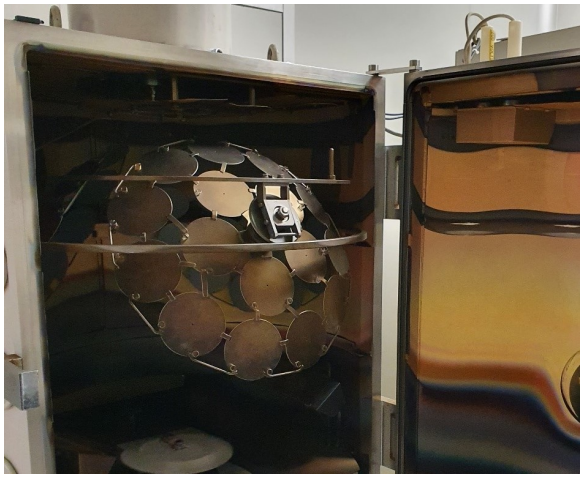

Figure 4.11: Evaporator support

After this process, the wafer was removed from the holder

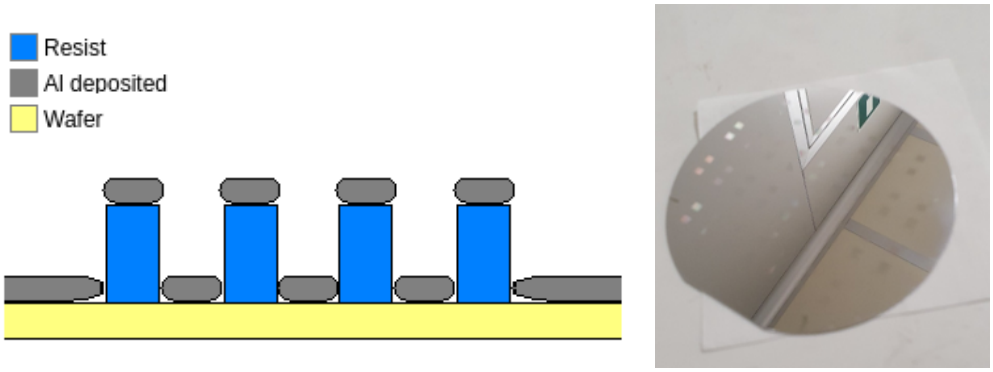

(a) **(b)**

Figure 4.12: (a) the wafer surface after the metal deposition, (b) metallized wafer

Now the Lift-Off technique is applied to remove excess material on the surface. To do this, an etching is made on the resist under the aluminum (Figure 4.12 (a)). The solvent used is "Remover PG" (N-Methyl Pyrrolidone). In this way the aluminum deposited on the resist can be peeled from the surface, leaving it only where it is needed.
The wafer is placed in a baker and immersed in the solvent, the use of heat and an ultrasonic bath speed up the process, helping the detachment of the aluminum from the surface.

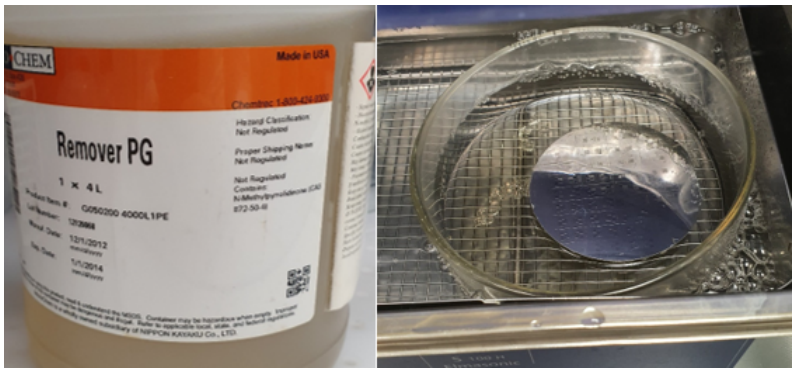

Figure 4.13: Liftoff process

The final result is shown below:

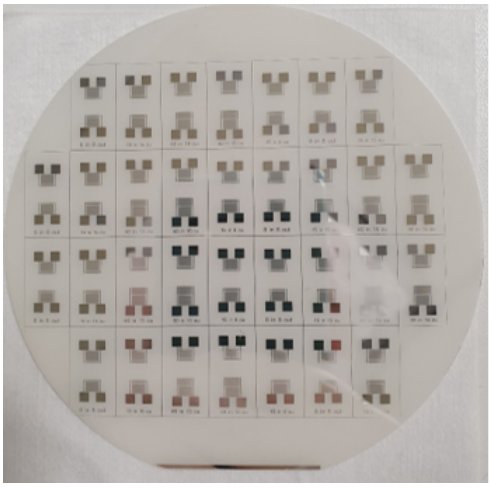

Figure 4.14: Wafer final result

Chapter 5

Device testing

A VNA (Vector Network Analyzer) was used to test the SAW devices made. This instrument is used to measure the scattering parameters of a generic DUT. A NanoVNA-H was used for the tests presented in this work. To obtain the graphs presented below, the NanoVNA device was connected to the PC and read by Matlab via the NanoVNA-MATLAB library (https://github.com/qrp73/NanoVNA-MATLAB). Due to the lack of a wire bonder machine, a special container was made to create electrical contacts with the pads of the SAW devices and do the measurements.

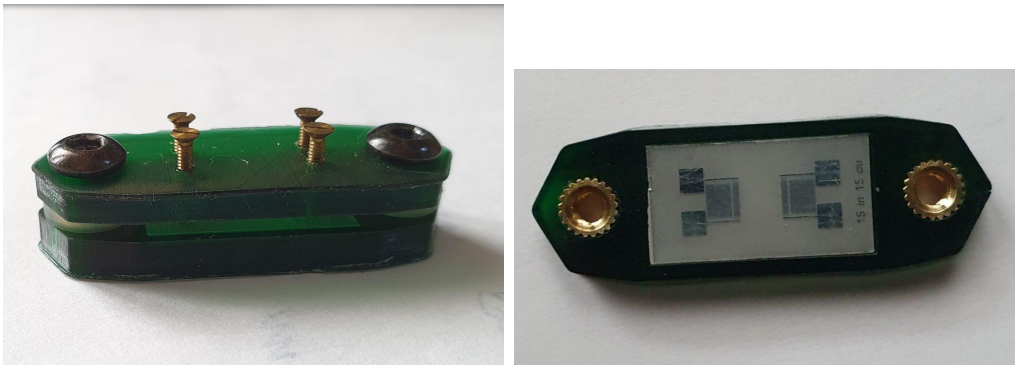

(a) **(b)**

Figure 5.1: (a) container closed with contact screws , (b) compartment that contains the SAW device

The screws shown in Figure 5.1 (a), when carefully adjusted, create electrical

contact between the pads and the SMA connectors used to interface the SAW device with the NanoVNA (Figure 5.2).

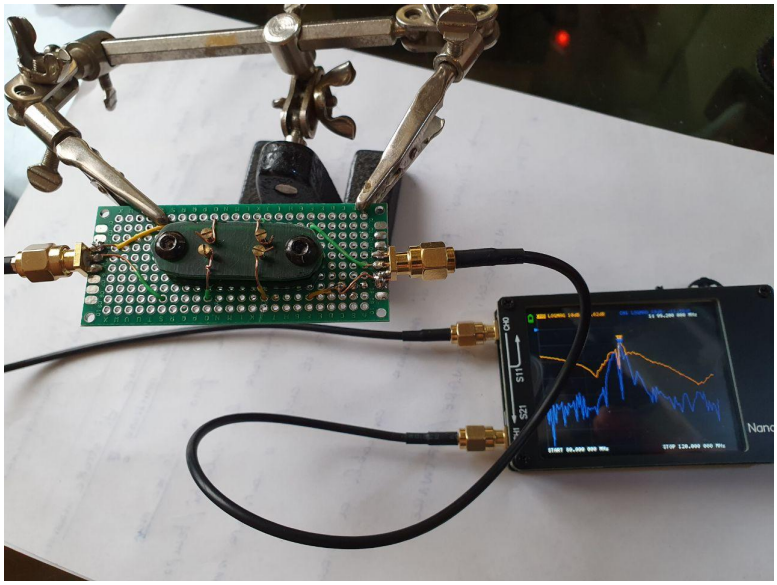

Figure 5.2: Connection between NanoVNA and a SAW device

Table 5.1 gives a summary of all tested devices. In this table, each device has been labeled working (W) or not working (NW) or damaged during testing (BR).

Device no.	Input	Output	dev. 1	dev. 2	dev. 3	dev. 4
1	8	8	BR	W	W	BR
2	15	8	W	NW	NW	BR
3	15	15	BR	W	W	W
4	40	15	NW	W	NW	NW
5	50	15	W	NW	W	NW

Table 5.1: Summary of tested devices

The following charts are presented for each device type in comparison to the simulation results.

5.1 8 fingers pairs at INPUT and 8 finger pairs at OUTPUT

Devices 1 and 4 were damaged by the screws which removed the aluminum from the contact pads, but these also worked as shown in Figure 5.4. The following graph (Figure 5.3) shows devices 2 and 3 in relation to the graph obtained from the MATLAB simulation. It is possible to observe that the behaviour of both devices is superimposed upon the simulation. The resonance peak of the 2 devices is reported to 99.2 MHz with respect to the simulation (100 MHz), this is because the "IDT MASK ELEMENT GENERATOR" program makes an approximation of the size of a and b in the IDTs (so, the same occurs for all devices).

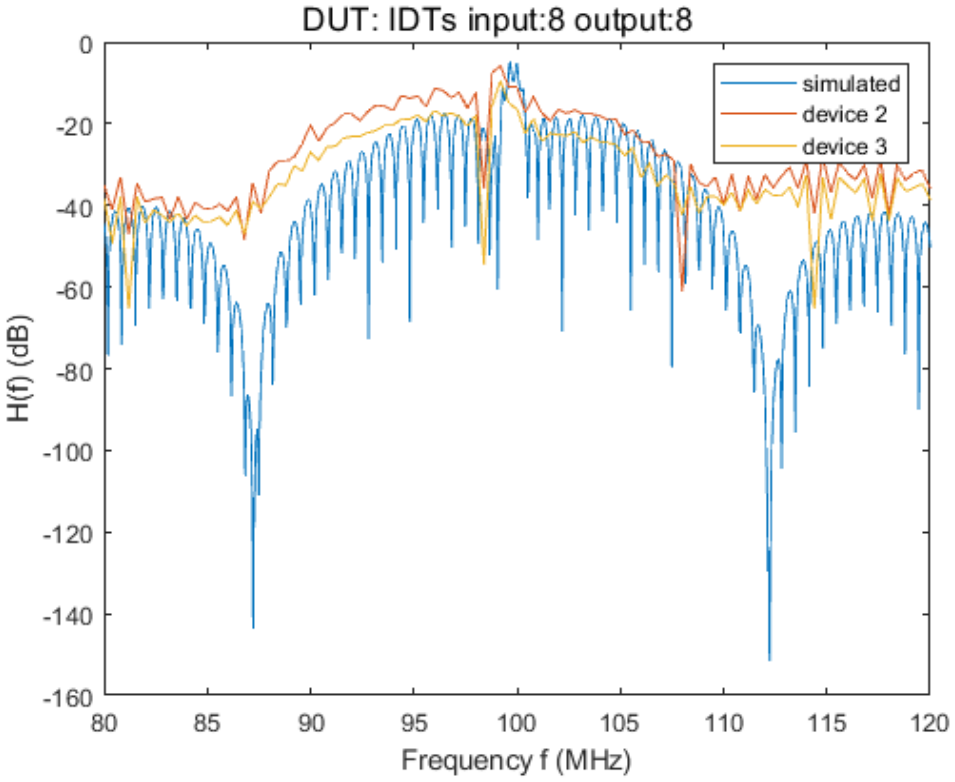

Figure 5.3: S_{21} : comparison between simulation and real devices

Performances obtained by the real devices are quite similar to the simulated one. That simulated on the center frequency introduces a loss of -5.3 dB, the device 2 -5.9 dB and the device 3 -9.5 dB (at 99.2 MHz). Below are reported the two graphs of the devices 1 and 4.

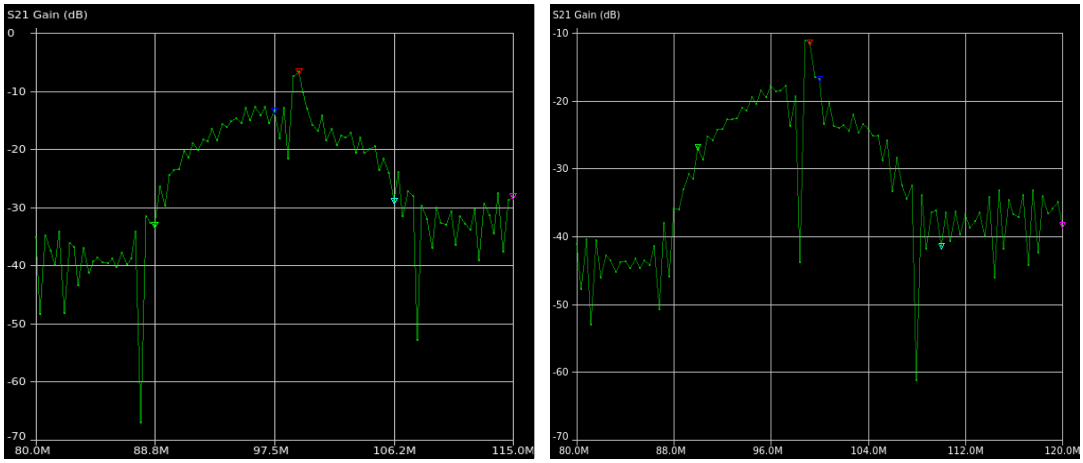

(a) **(b)**

Figure 5.4: (a) device 1 , -6.54 dB at resonance 99.2MHz , (b) device 4 , -10.98dB dB at resonance 98.9MHz

5.2 15 fingers pairs at INPUT and 8 finger pairs at OUTPUT

Only one of these devices is working, the others are not working because of the aluminum residue after the lift-off process. The same considerations made earlier are still applicable to this device: the center frequency is reported at 99.2 MHz, but the overall response is almost the same as the simulation.

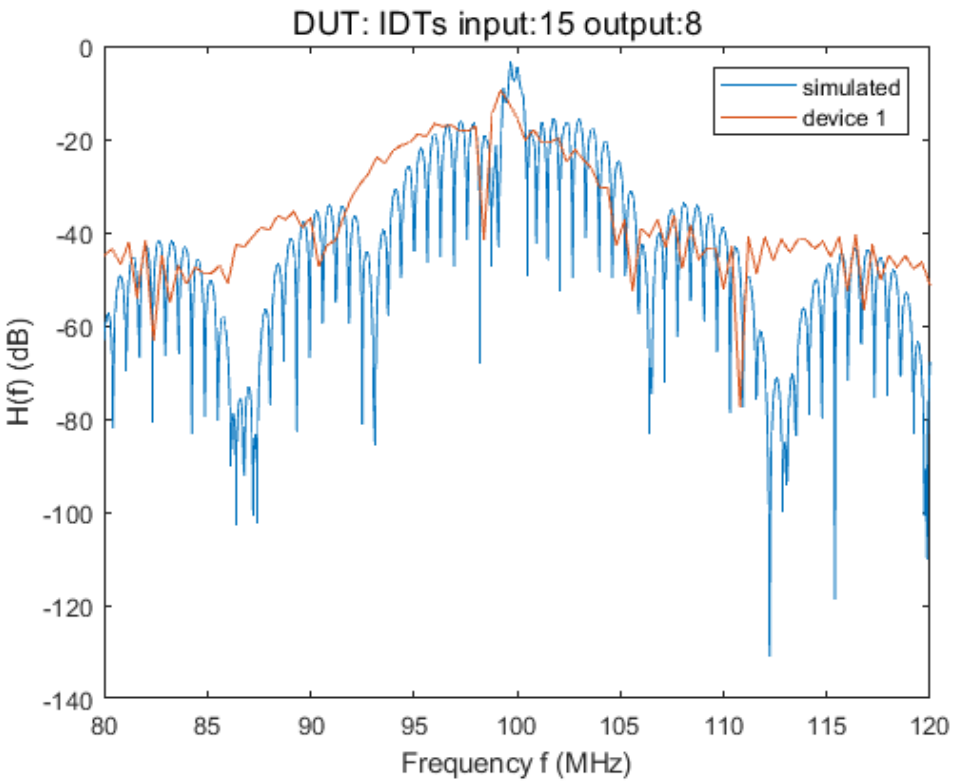

Figure 5.5: S_{21} dB response of device 1 compared with the simulation. At resonance device 1 shows an attenuation of -9.56 dB (99.2MHz) meanwhile the simulated one -4.59 dB (100MHz)

5.3 15 fingers pairs at INPUT and 15 finger pairs at OUTPUT

The pads of device 1 were damaged by screws in the contact points. Figure 5.7 shows the device 1 response. The Figure 5.6 shows the response of devices 2,3 and 4.

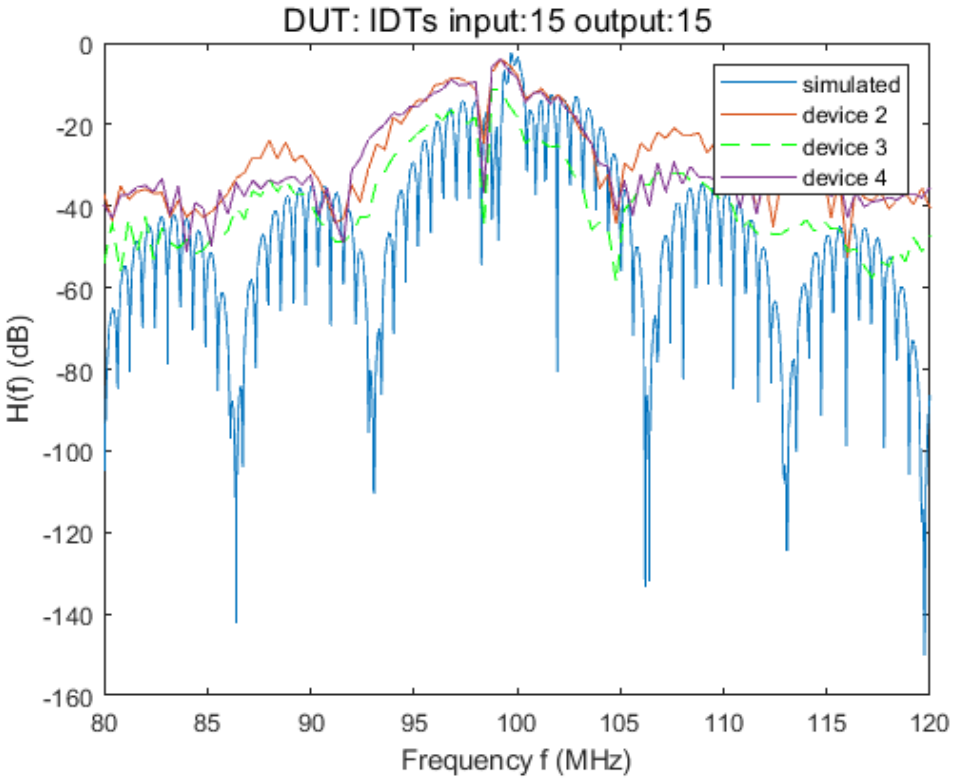

Figure 5.6: S_{21} dB response of devices 2,3,4 compared with the simulation. At resonance (99.2MHz) S_{21} for devices 3,4 is -3.98 dB, for device 4 is -11.48 dB and the simulated one is -3.79 dB (resonance 100MHz)

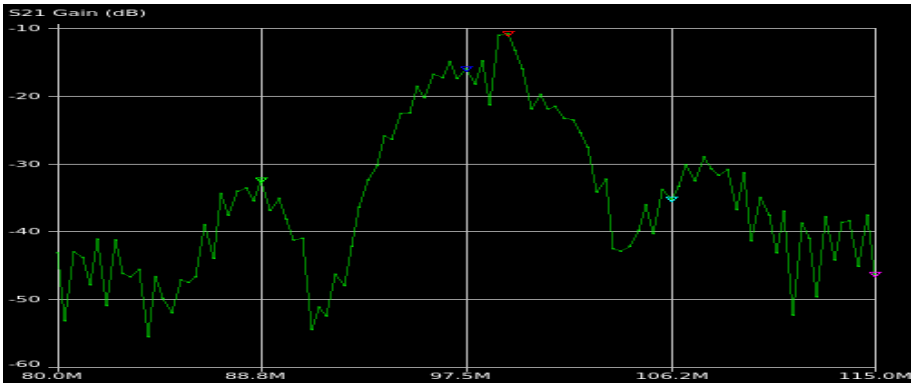

Figure 5.7: S_{21} dB response of device 1. At resonance (99.2 MHz) S_{21} is -10.81 dB

5.4 40 fingers pairs at INPUT and 15 finger pairs at OUTPUT

The dashed line in Figure 5.8 for device 1 represents an incorrect behavior. This device behaves like a SAW resonator with approximately 15 pairs of fingers for input and output, so it has been labelled NW (not working); the cause could be related to a damage to the pairs of IDT fingers at the input. Devices 3 and 4 did not work at all, due to a damage to the IDTs during the Lift-Off process.
Device 2 provides a good approximation of the simulated response, but has high losses compared to the other devices: S_{21} at 99.2MHz is -14 dB instead of -3.32 dB for the simulated one.

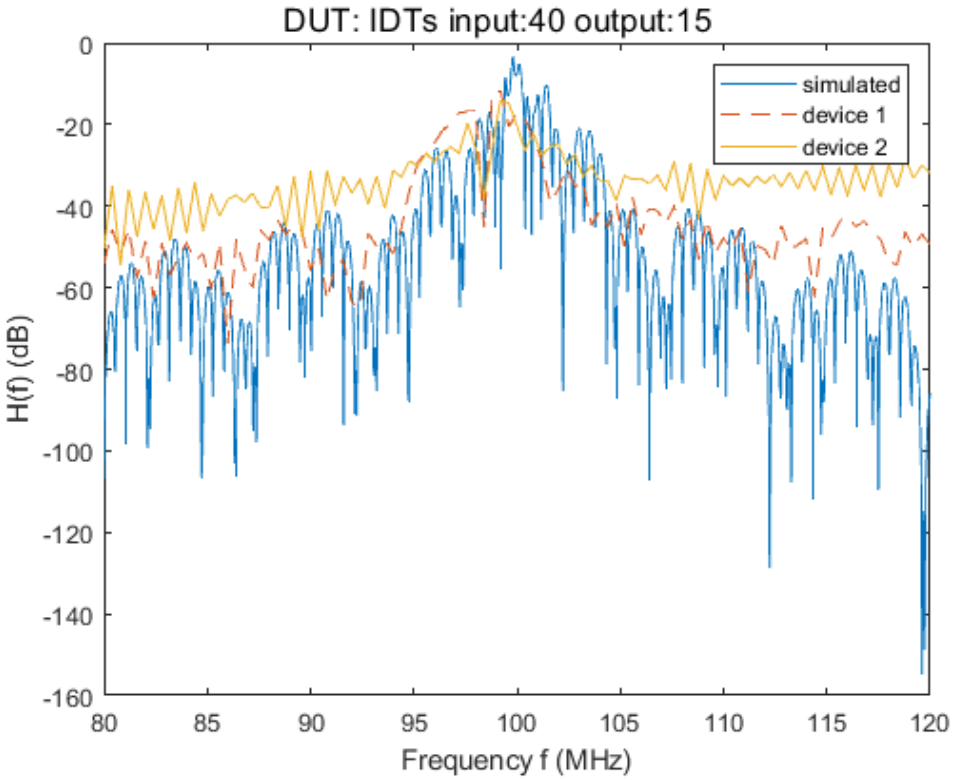

Figure 5.8: S_{21} response of device 1 and device 2

5.5 50 fingers pairs at INPUT and 15 finger pairs at OUTPUT

The dashed line in Figure 5.9 for device 1 represents the incorrect behaviour, the comment is identical to the one in the previous section. Device 1 shows two resonant peaks near the center frequency, they are also present in the simulation but are closer to the center frequency which appears as a single peak. Probably the distance between the two peaks in the actual device is due to some tolerance in the production process. These two peaks are symmetric to the center frequency 99.2MHz, the first can be found at 98.8 MHz and the second one at 99.6 MHz and both introduce a loss of -8 dB, at the center frequency the S_{21} is -13.22 dB. Device 3 behaves correctly as the simulation, but it introduces high losses at the center frequency (99.2 MHz) -19 dB instead of -4.1 dB at 100 MHz.

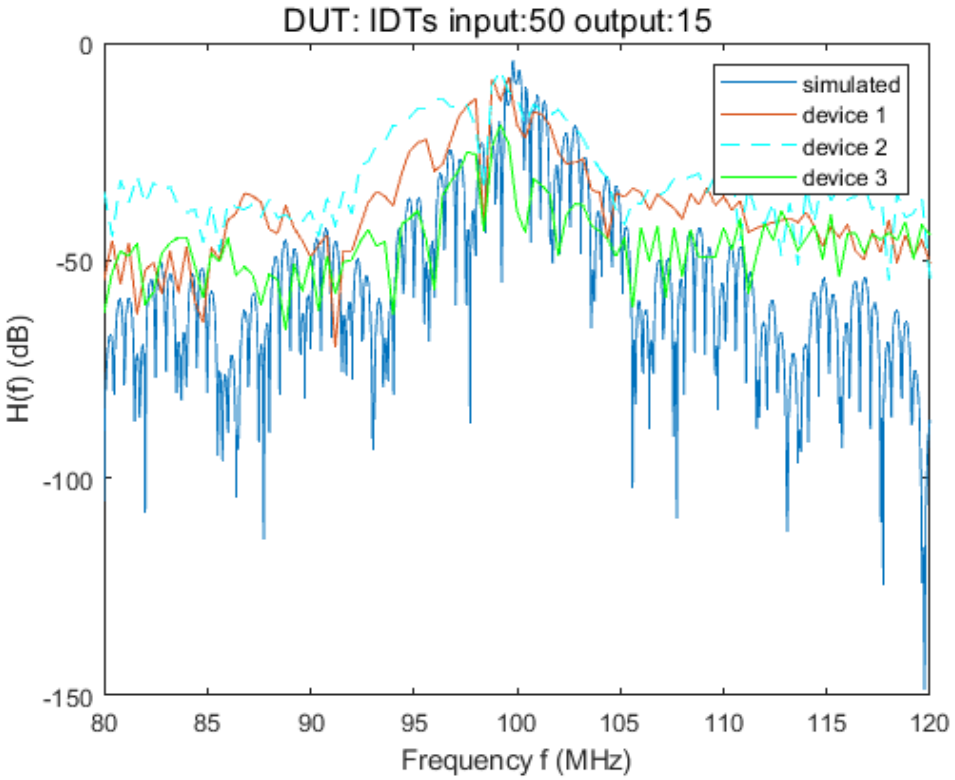

Figure 5.9: S_{21} response of device 2 and device 3 and 4

5.6 Conclusions

Among all the devices made, only a few showed values very similar to those obtained from the simulations, both in terms of S_{21} gain and in terms of reproducibility of the measurements. This refers to devices in sections 5.3 (dev. 2 and dev. 4) and 5.1 (dev. 2 and dev. 3). These will be used to attempt to implement a SAW transponder as a measurement system.
Another comment can be done on the test bench. Changing the way electrical contacts are made reduces the risk of damage to the DUT (device under test) PADs, therefore for the final implementation the container shown in Figure 5.1 will be modified to use the POGO pins (spring loaded connector) instead of the screws. Implementing this type of contact also improves the quality of the electrical contact by reducing any parasitic effects related to the signal transmission line.

(a)

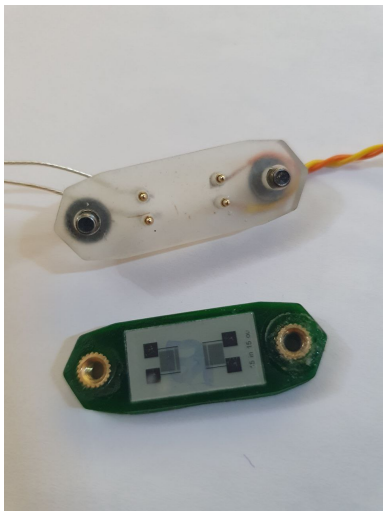

(b)

Figure 5.10: (a) POGO pin: gold plated copper (b) container lid with POGO pins

Chapter 6

Testing sensor-transponder configuration

In this chapter the transponder-sensor configuration is tested to roughly evaluate the quality of the obtainable measurements. In the Figure 6.1 is reported the configuration used.

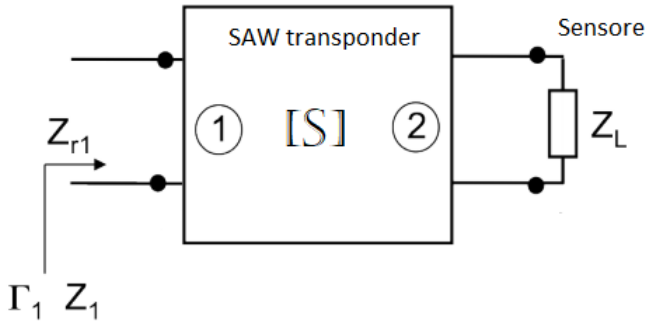

Figure 6.1: SAW transponder connected with the sensor

A temperature sensor (PT100) was chosen to conduct this test. This sensor is a thermistor and it has a linear characteristic with the temperature for a temperature range between -10°C and 350°C that is $R_L(T) = 100\Omega \cdot (1 + 0.004 \cdot T)$.
A change in temperature changes the resistance of the sensor. Then the load reflection coefficient and also the amount of reflected signal change. This can be

evaluated at the input port of the device by the scattering matrix relation:

$$S'_{11} = S_{11} + \frac{S_{21} \cdot S_{12} \cdot \Gamma_L}{1 - S_{22} \cdot \Gamma_L} \tag{6.1}$$

The SAW device has a reference impedance of $Z_{r1} = 50\Omega$. The device used is the *device 2* reported in the section 5.3. It is symmetrical and reciprocal ($S_{11} = S_{22}$ and $S_{21} = S_{12}$) and it works at 99.2 MHz, so $|S_{11}| = -9.69$dB and $|S_{21}| = -3.98$dB.

$$\Gamma_L(T) = \frac{R_L(T) - Z_{r1}}{R_L(T) + Z_{r1}} \tag{6.2}$$

Measurements were performed on NanoVNA (introduced in chapter 5). The measured value is the return loss (RL).

$$RL = 20 \cdot log_{10}(S'_{11}) \tag{6.3}$$

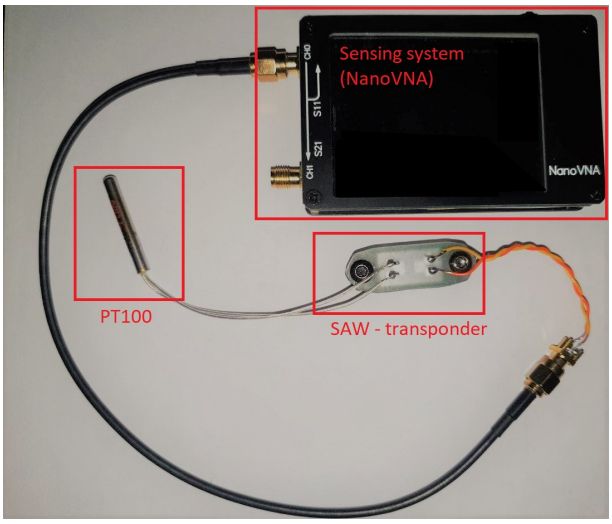

Figure 6.2: Sensing system: PT100, SAW transponder and NanoVNA

To improve the resolution of the NanoVNA's Return Loss channel, the measuring device has been set to have a minimum sweep around the working frequency: center 99.2MHz and span 100kHz. In this way it is possible to measure RL correlated with the PT100 with the maximum instrument resolution (1 kHz/step).
In the figure below (Figure 6.3) are reported the experimental results compared with the simulation. The experiment was conducted by making 35 measurements for each temperature step (25 total steps verified with a thermocouple probe). In the table below (Table 6.1) are reported the temperature steps and the averaged RL values obtained.

Temp	**1°C**	**24°C**	**31°C**	**34°C**	**37°C**	**39°C**	**40°C**	**43°C**	**44°C**
RL (dB)	-9.120	-8.433	-8.296	-8.233	-8.178	-8.075	-8.048	-7.862	-7.830
Temp	**47°C**	**48°C**	**50°C**	**51°C**	**102°C**	**110°C**	**129°C**	**167°C**	**168°C**
RL (dB)	-7.559	-7.534	-7.377	-7.350	-5.917	-5.876	-5.615	-5.212	-5.206
Temp	**190°C**	**191°C**	**200°C**	**217°C**	**220°C**	**242°C**	**257°C**		
RL (dB)	-4.968	-4.960	-4.827	-4.608	-4.587	-4.365	-4.196		

Table 6.1: Measurement summary

The transponder is kept at a constant temperature of 24 degrees Celsius.

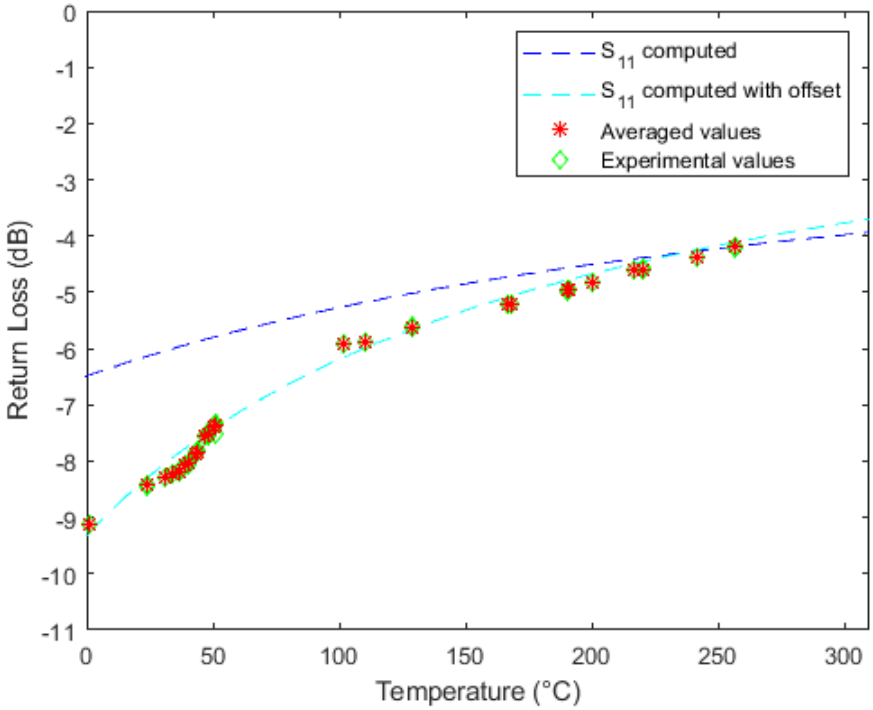

Figure 6.3: Measured characteristic on temperature change

In Figure 6.3 it is possible to observe that the device behaves almost as in the simulation. It is necessary to provide both a horizontal and vertical offset to the theoretical curve (blue dashed line in Figure 6.3) for a correct approximation of the experimental data . The cyan dashed curve is obtained applying a horizontal offset $\mathrm{T}_{off} = 139°\mathrm{C}$ and a vertical offset $\mathrm{RL}_{off} = 1\mathrm{dB}$.

$$\mathrm{RL}_c(\mathrm{T} - \mathrm{T}_{off}) = 20 \cdot log_{10}(S'_{11}(\mathrm{T} - \mathrm{T}_{off})) + \mathrm{RL}_{off} \tag{6.4}$$

Thanks to these corrections the theoretical curve approximates the experimental

data with a relative error of 4%. To achieve a simpler relation between temperature and Return Loss, two different approximations are made: linear approximation (section 6.1) and quadratic approximation (section 6.2).

6.1 Linear approximation

For the linear approximation two regression lines were implemented. Using MATLAB it is possible to fit the experimental data and obtain the corresponding best fitting line. In the figure below (Figure 6.3) it is shown the result of this process.

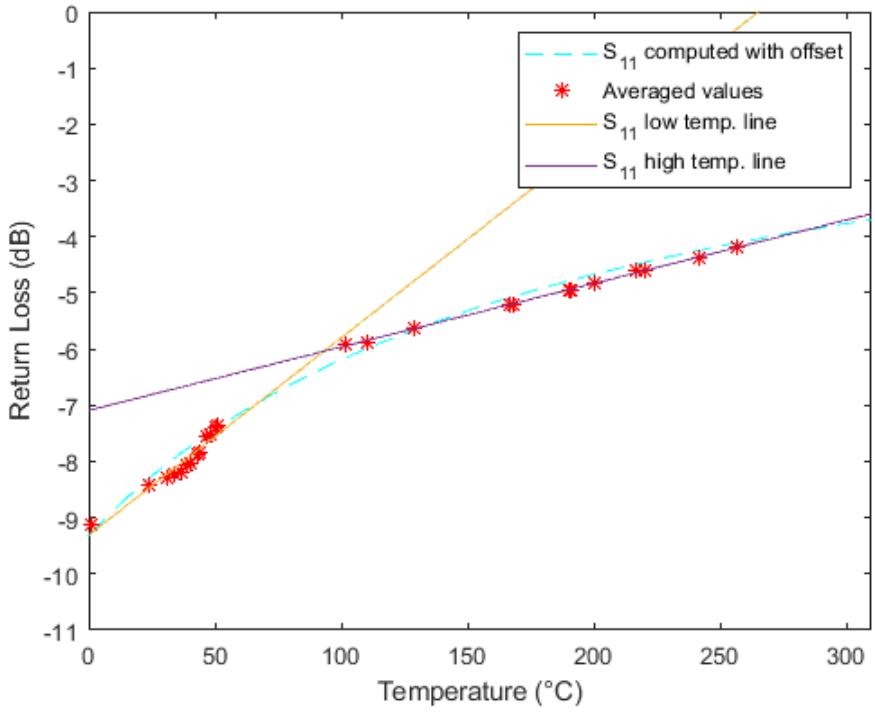

Figure 6.4: The two $RL(T)$ approximated characteristics on temperature change

The relations between the Return Loss and the temperature are:

$$RL(T)\Big|_{dB} = 0.0351 \cdot T\Big|_{^oC} - 9.31 \text{ dB for T} \leq 92°\text{C} \tag{6.5}$$

$$RL(T)\Big|_{dB} = 0.0113 \cdot T\Big|_{^oC} - 7.09 \text{ dB for T} > 92°\text{C} \tag{6.6}$$

These produce uncertainty in reading that is equal to ±3 % in the range 0°C ÷ 50°C (estimated from experimental values), less than ±5% in range 50°C ÷ 92°C (estimated by comparing the theoretical curve and the approximating line) and ±1% in the range 93°C ÷ 260°C (estimated from experimental values).
Considering only one regression line approximating the full temperature range 0°C ÷ 260°C the equation is

$$RL(T)\Big|_{dB} = 0.0191 \cdot T\Big|_{^oC} - 8.62 \text{ dB} \tag{6.7}$$

and the relative error is ±12%.

6.2 Quadratic approximation

The same procedure done in the section 6.1 is repeated to obtain the quadratic approximation curve. This covers all the temperature range 0°C ÷ 260°C with a unique relationship between temperature and RL. Below in the Figure 6.4 is reported the result.

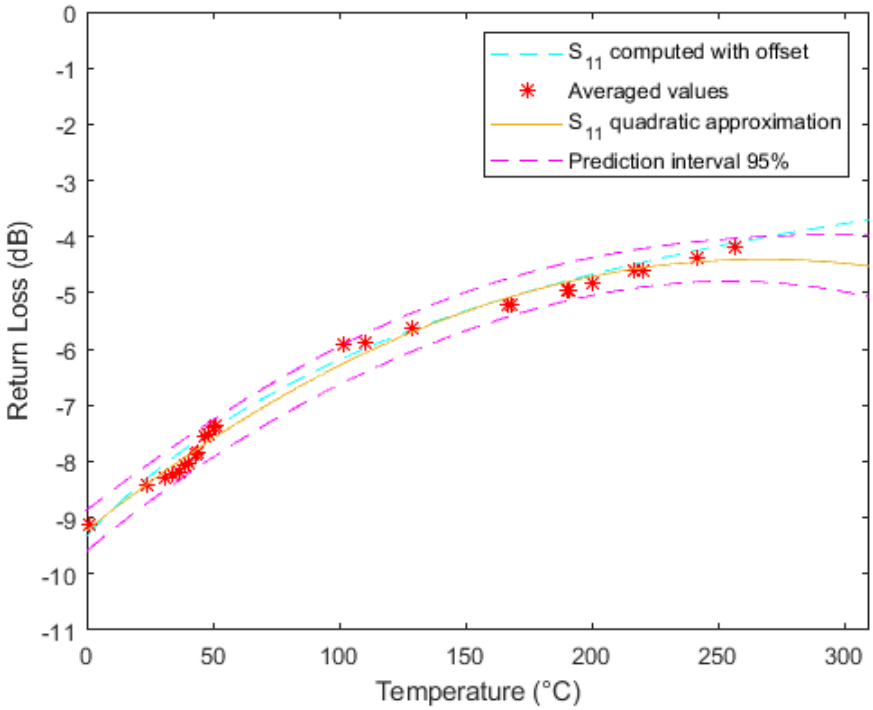

Figure 6.5: Approximated characteristic on temperature change

The relation between the Return Loss and the temperature is:

$$RL(T)\Big|_{dB} = -6.7 \cdot 10^{-}5 \cdot T^2\Big|_{.^oC} + 0.036 \cdot T\Big|_{.^oC} - 9.23 \text{ dB} \tag{6.8}$$

This approximation produces uncertainty in reading that is ±5.6% (estimated from experimental values).

6.3 Conclusions

This experiment demonstrated the possibility of measuring an external sensor connected to a Two-Port SAW resonator. The behaviour of the system is predictable and stable, as illustrated in Figure 6.3. The RL-Temperature converting error, using the theoretical curve (equation 6.4), is 4%. The development of the models in sections 6.1 and 6.2 was required to obtain simpler relations in the calculation of the RL-Temperature conversion. The best derives from the quadratic approximation (section 6.2). This result has a relative reading error that is less than 6% and covers all the temperature range with the same relation (equation 6.8). The linear approximation is more precise but requires two different equations which considers two different temperature range (equation 6.5) and (equation 6.6) which produce respectively a relative error of ±3% and ±1%.
The measurements presented were made using a wired connection with the VNA. In the case of a wireless measurement other factors must be considered: the losses due to the signal attenuation caused by the distance between transmitter and transponder and the losses introduced by the use of antennas (not all the power received by the antenna is transformed into a signal: so antenna the gain). The power received P_{rx} by the interrogation unit, after an interrogation, is given by the radar equation (from the radar theory)[14]:

$$P_{rx} = \frac{P_{tx} G^2 \sigma \lambda^2}{(4\pi)^2 R^4} \tag{6.9}$$

Where P_{tx} is the transmitted power, G is the antenna gain for the receiver and the transmitter. λ is the electromagnetic wavelenght, R is the distance betwen the transponder and the interrogation unit. σ is the RCS (radar cross-section) this contains the $RL(T)$

$$\sigma \stackrel{\text{def}}{=} \frac{\text{reflected power}}{\text{incident power}} \approx G_{dut}^2 \cdot 10^{RL(T)/20} \tag{6.10}$$

where G_{dut} is the antenna gain of the transponder.

Here below is reported the curve Rx power vs temperature of a hypothetical interrogation unit (IU) which has a Tx Power of 2W and an antenna gain of 7dBi and a SAW transponder with an antenna gain of 1 dBi. The distance between IU and transponder is 4 m.

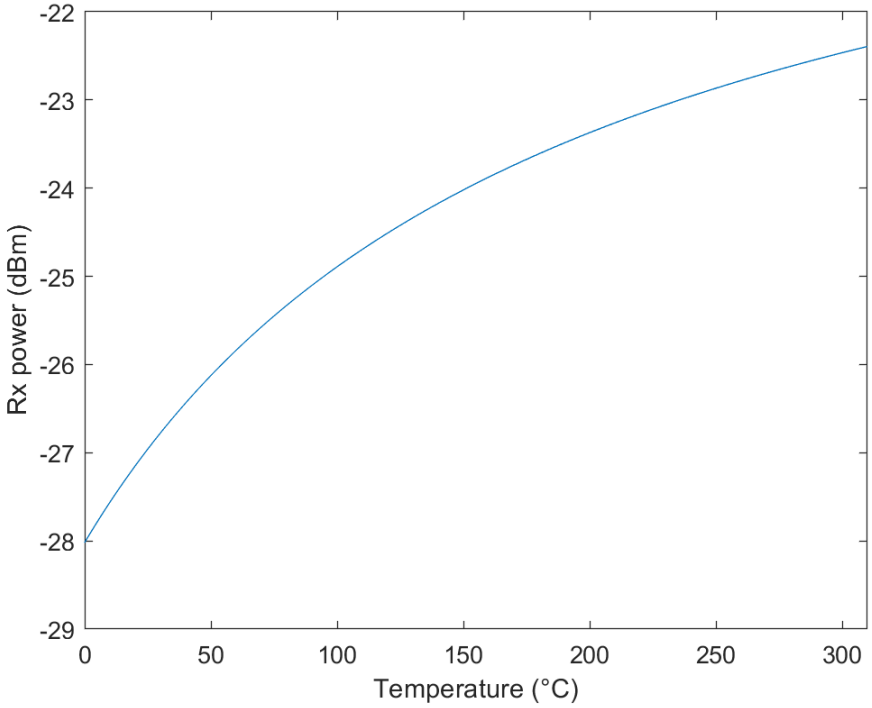

Figure 6.6: Received power from SAW transponder after an interrogation. The power is measured in dBm, $1dB = 10 \cdot \log(1W/1mW) = 30dBm$

Appendix A

Matematical models

A.1 Delta function model

$$H_1(f) = \sum_{n=-(N-1)/2}^{(N-1)/2} (-1)^n A_n e^{j\beta x_n} \tag{A.1}$$

Where the value $(-1)^n$, as previously said, represents the alternate polarity of the electric field, the term A_n represents the overlapping region between two electrodes.

$$H_1(f) = \sum_{n=-(N-1)/2}^{(N-1)/2} (-1)^n A_n[\cos \beta x_n - j \sin \beta x_n] \tag{A.2}$$

Choosing the reference axis x=0 in the center of the IDT, the summation results in a simplification of the all sine components in the expression thanks to the following trigonometric relation: $\cos(\theta) = \cos -\theta$ and $\sin(-\theta) = -\sin(\theta)$. The value of A_n is fixed to one and using one delta approximation per IDT, this means that every electrode is represented by one delta function in the center so $\eta = 1$, every delta is distant from another of the fixed quantity $\lambda_0/2$.

$$H_1(f) = A_n \sum_{n=-(N-1)/2}^{(N-1)/2} (-1)^n \cos \beta x_n \tag{A.3}$$

$$\beta x_n = \frac{2\pi f}{v_{saw}} \cdot n \cdot a = \frac{2\pi f}{v_{saw}} \cdot n \cdot \frac{\lambda_0 \eta}{2} = \frac{2\pi f}{v_{saw}} \cdot n \cdot \frac{v_{saw}\eta}{2f_0} = \pi n \cdot \frac{f}{f_0} \cdot \eta = \pi n \cdot \frac{f}{f_0} \tag{A.4}$$

Substituting f with $(f - f_0) + f_0$:

$$\beta x_n = \pi n \cdot \frac{f - f0}{f_0} + \pi n \tag{A.5}$$

$$\cos \beta x_n = \cos \left(\pi n \cdot \frac{f - f0}{f_0} + \pi n\right) = (-1)^n \cdot \cos \left(\pi n \cdot \frac{f - f0}{f_0}\right) \tag{A.6}$$

So the transfer function assumes the following form:

$$\begin{aligned} H_1(f) = A_n \sum_{n=-(N-1)/2}^{(N-1)/2} (-1)^n \left((-1)^n \cdot \cos \left(\pi n \cdot \frac{f - f0}{f_0}\right)\right) = \\ A_n \sum_{n=-(N-1)/2}^{(N-1)/2} \cos \left(\pi n \cdot \frac{f - f0}{f_0}\right) \end{aligned} \tag{A.7}$$

because $\cos(-\theta) = \cos(\theta)$ it is possible to reduce the calculation between $0 \rightarrow (N-1)/2$

$$H_1(f) = 2A_n \cdot \sum_{n=0}^{(N-1)/2} \cos \left(\pi n \cdot \frac{f - f0}{f_0}\right) \tag{A.8}$$

if $A_n = 1$ then:

$$H_1(f) = 1 + 2\cos \left(\pi \cdot \frac{f - f0}{f_0}\right) + 2\cos \left(2\pi \cdot \frac{f - f0}{f_0}\right) + ... + 2\cos \left(N_p \pi \cdot \frac{f - f0}{f_0}\right) \tag{A.9}$$

Where N_p has the following value:

$$N_p^{odd} = \frac{N-1}{2} \approx \frac{N}{2} \tag{A.10}$$

$$N_p^{even} = \frac{N}{2} \tag{A.11}$$

The expression of the transfer function may be approximated with a $sinc(x)$ as shown below

$$X = N_p \pi \cdot \frac{f - f0}{f_0} \tag{A.12}$$

$$|H_1(f)| \propto \left|\frac{\sin X}{X}\right| = \left|\frac{\sin N_p\pi \cdot \frac{f-f0}{f_0}}{N_p\pi \cdot \frac{f-f0}{f_0}}\right| \tag{A.13}$$

Appendix B

Source code

This code is used to test each device and to obtain the figures from (3.4) to (3.7)

content/code/main.m

```
clear all
close all
format longe
%rf system center frequency
f0= 100e6;
delta = 0.2;
resolution = 1025;
%window = linspace(f0*(1-delta)+10e6,f0*(1+delta)-10e6,resolution);
window = linspace(f0*(1-delta),f0*(1+delta),resolution);
window1 = linspace(f0*(1-delta),f0*(1+delta),101);
%material main parameters: LiNbO3 YZ cut
material.epsR = 42.3;
material.K2 = 0.045;
material.C0 = 4.5e-12; %pF/cm
material.Vs = 3488; %m/s
material.k11p = 0.0018;
material.k11m = 0.30;
material.k11s = 0;
material.k12p = 0.0054;
material.k12m = 0.08;
material.k12s = 0;
material.loss = 0.00045;
%constructive parameters for the IDT
constructive_parameters.h = 100e-9; % height of metallization
constructive_parameters.b = 0.5; %b = 0.5 #unit of lambda
constructive_parameters.eta = 0.5;% aspect ratio a/b
constructive_parameters.W = 80; % unit of lambda (Apodization)
```

```
constructive_parameters.Rs = 50;%22.3-12.7j;
constructive_parameters.Ze = 50;
%Call to class
saw = SAWsolver(f0);
saw.load_material_param(material);
saw.IDT_load_parameters(constructive_parameters);
n=1;

Nin  = 100; % number of finger for input  IDT
Nout = 30;% number of finger for output IDT

for f=window

    %input idt
    params = struct('Nt',Nin, 'f',f, 'role',"input");
    IDT_in = saw.CreateSawObject('T', params);
    %output idt
    params = struct('Nt',Nout, 'f',f, 'role',"output");
    IDT_ou = saw.CreateSawObject('T', params);
    %grating
    params = struct('Nt',60, 'f',f, 'role',"element", 'theta_ref',0);
    G = saw.CreateSawObject('G', params);
    %spacers
    clear param % removing data from param
    %n = 5;
    %params = struct('role',"element", 'f',f, 'Ls',saw.material.
    lambdaS*(m/2+1/8), 'dist_type',"lenght");
    params = struct('role',"element", 'f',f, 'Ls',saw.material.
    lambdaS*3.6, 'dist_type',"lenght");
    Dg = saw.CreateSawObject('D', params); %grating spacer
    params.Ls = 1e-6; %1 us delay
    params.dist_type = "time";
    Ds = saw.CreateSawObject('D', params); %idt spacer

    M = G.Tn*Dg.Tn*IDT_in.Tn*Ds.Tn*IDT_ou.Tn*Dg.Tn*G.Tn;
    N = G.Tn*Dg.Tn*IDT_in.Bn;
    L = (IDT_in.Cn*Ds.Tn*IDT_ou.Tn*Dg.Tn*G.Tn);
    H_inou(n) = 1/M(1,1)*(IDT_ou.Cn*Dg.Tn*G.Tn)*G.Tn*Dg.Tn*IDT_in.Bn;

    S11(n) = L(1)*(-N(1)/M(1,1))+IDT_in.t33n;

    VSWR(n) = (1+abs(S11(n)))/(1-abs(S11(n)));

    n = n+1;
end
%plot(window*1e-6, 20*log10(abs(H_inou)))
% IDT 8 in 8 ou
% S_rd2 = sparameters("misure/8x8/dev2.s2p").Parameters(2,1,:);
% S_rd3 = sparameters("misure/8x8/dev3.s2p").Parameters(2,1,:);
```

```
75 %
76 % figure(1);
77 % plot(window*1e-6, 20*log10(abs(H_inou)))
78 % hold on
79 % plot(window1*1e-6,20*log10(abs(S_rd2(:))))
80 % hold on
81 % plot(window1*1e-6,20*log10(abs(S_rd3(:))))
82 % legend('simulated','device 2', 'device 3')
83 % xlabel("Frequency f (MHz)")
84 % ylabel("H(f) [dB]")
85 % sgtitle(strcat('DUT: IDTs input: ',int2str(Nin/2),' output: ',
       int2str(Nout/2)))
86
87 % IDT 15 in 15 ou
88 % S_rd2 = sparameters("misure/15x15/dev2.s2p").Parameters(2,1,:);
89 % S_rd3 = sparameters("misure/15x15/dev3.s2p").Parameters(2,1,:);
90 % S_rd4 = sparameters("misure/15x15/dev4.s2p").Parameters(2,1,:);
91 %
92 % figure(1);
93 % plot(window*1e-6, 20*log10(abs(H_inou)))
94 % hold on
95 % plot(window1*1e-6,20*log10(abs(S_rd2(:))))
96 % hold on
97 % plot(window1*1e-6,20*log10(abs(S_rd3(:))),'g--')
98 % hold on
99 % plot(window1*1e-6,20*log10(abs(S_rd4(:))));
100 % legend('simulated','device 2','device 3','device 4')
101 % xlabel("Frequency f (MHz)")
102 % ylabel("H(f) [dB]")
103 % sgtitle(strcat('DUT: IDTs input: ',int2str(Nin/2),' output: ',
       int2str(Nout/2)))
104
105 % IDT 15 in 8 ou
106 % S_rd1 = sparameters("misure/15x8/dev1.s2p").Parameters(2,1,:);
107 %
108 % figure(1);
109 % plot(window*1e-6, 20*log10(abs(H_inou)))
110 % hold on
111 % plot(window1*1e-6,20*log10(abs(S_rd1(:))));
112 % legend('simulated','device 1')
113 % xlabel("Frequency f (MHz)")
114 % ylabel("H(f) [dB]")
115 % sgtitle(strcat('DUT: IDTs input: ',int2str(Nin/2),' output: ',
       int2str(Nout/2)))
116
117 %IDT 40 in 15 ou
118 % S_rd2 = sparameters("misure/40x15/dev2.s2p").Parameters(2,1,:);
119 % S_rd1 = sparameters("misure/40x15/dev1.s2p").Parameters(2,1,:);
120 %
```

```
% figure(1);
% plot(window*1e-6, 20*log10(abs(H_inou)))
% hold on
% plot(window1*1e-6,20*log10(abs(S_rd1(:))),'--')
% hold on
% plot(window1*1e-6,20*log10(abs(S_rd2(:))));
% legend('simulated','device 1','device 2')
% xlabel("Frequency f (MHz)")
% ylabel("H(f) [dB]")
% sgtitle(strcat('DUT: IDTs input: ',int2str(Nin/2),' output: ',
    int2str(Nout/2)))

%IDT 50 in 15 ou
S_rd1 = sparameters("misure/50x15/dev1.s2p").Parameters(2,1,:);
S_rd2 = sparameters("misure/50x15/dev2.s2p").Parameters(2,1,:);
S_rd3 = sparameters("misure/50x15/dev3.s2p").Parameters(2,1,:);

figure(1);
plot(window*1e-6, 20*log10(abs(H_inou)),'-')
hold on
plot(window1*1e-6,20*log10(abs(S_rd1(:))),'-')
hold on
plot(window1*1e-6,20*log10(abs(S_rd2(:))),'c--')
hold on
plot(window1*1e-6,20*log10(abs(S_rd3(:))),'g-');
legend('simulated','device 1','device 2','device 3')
xlabel("Frequency f (MHz)")
ylabel("H(f) [dB]")
sgtitle(strcat('DUT: IDTs input: ',int2str(Nin/2),' output: ',int2str
    (Nout/2)))
```

This is the class that permits to solve a saw circuit and to create saw object using transmission matrix model.

content/code/SAWsolver.m

```
classdef SAWsolver < handle
    properties
        eps0 = 8.85418781762e-12;
        c = 3e8;
        f0 = 0;
        material = struct();
        idt = struct();
    end
    methods

        function obj = SAWsolver( center_frequency )
            obj.f0 = center_frequency;
        end
```

```
14
15          % MATERIAL PROPERTIES
16
17          function load_material_param(obj, material)
18              obj.material = material;
19              obj.material.lambdaS = obj.material.Vs/obj.f0;
20              obj.material.beta = 2*pi/obj.material.lambdaS;
21          end
22
23          %IDT PROPERTIES
24
25          function IDT_load_parameters(obj, constructive_parameters)
26
27              obj.idt.h = constructive_parameters.h;
28              obj.idt.h_lambda = obj.idt.h/obj.material.lambdaS;
29
30              obj.idt.b = 17e-6;%constructive_parameters.b*obj.material
    .lambdaS;
31              obj.idt.a = 9e-6;%constructive_parameters.eta*obj.idt.b;
32              obj.idt.W = constructive_parameters.W*obj.material.
    lambdaS*100; % *100 converts um to cm
33              obj.idt.Cs = obj.idt.W*obj.material.C0;
34
35              obj.idt.Rs = constructive_parameters.Rs;
36              obj.idt.Ze = constructive_parameters.Ze;
37
38              obj.idt.G0 = obj.material.K2*obj.idt.Cs*obj.f0;
39              obj.idt.Z0 = 1/obj.idt.G0;
40
41              k11a = obj.material.k11p+obj.material.k11m*(obj.idt.h/obj
    .material.lambdaS)+obj.material.k11s*(obj.idt.h/obj.material.
    lambdaS)^2;
42              k12a = obj.material.k12p+obj.material.k12m*(obj.idt.h/obj
    .material.lambdaS)+obj.material.k12s*(obj.idt.h/obj.material.
    lambdaS)^2;
43
44              obj.idt.k11 = obj.material.beta*k11a;
45              obj.idt.k12 = obj.material.beta*k12a;
46
47              obj.idt.fa = (obj.material.Vs*(1-k11a))/obj.material.
    lambdaS;          % Average shifted velocity
48              obj.idt.fm = (obj.f0*obj.idt.fa)/(2*obj.f0-obj.idt.fa); %
     frequenza centrale sulla metallizzazione
49
50              obj.idt.Gm = (obj.material.K2*obj.idt.Cs*obj.idt.fm); %
    Impedenza caratteristica della metallizzazione
51              obj.idt.Zm = 1/obj.idt.Gm;
52
53          end
```

```
54
55          %computation
56          function circuit = solve(obj, circuit_input , input )
57              index = 1;
58              circuit_array = circuit_input;
59              for el = circuit_array
60                  if el.role == "input"
61                      el.Vin = input;
62                      vect = [el.Tn, el.Bn; el.Cn, el.t33n]*[el.O_Waves
    ; el.Vin];
63                      el.I_Waves = vect(1:2);
64                      el.Vou     = vect(3);
65                      %boundary starting conditions
66                      el.I_Waves = el.I_Waves.*[0;1];
67                      el.Vin = 0;
68                      circuit_array(index) = el;
69                      break
70                  end
71                  index = index +1;
72              end
73              %calculating saw waves due to input voltage to x = 0
74              next = index;
75              for i=2:index
76                  circuit_array(next-1).O_Waves = circuit_array(next).
    I_Waves;
77                  vect = [ circuit_array(next-1).Tn, circuit_array(next
    -1).Bn;
78                           circuit_array(next-1).Cn, circuit_array(next
    -1).t33n
79                          ]*[circuit_array(next-1).O_Waves;
    circuit_array(next-1).Vin];
80                  circuit_array(next-1).I_Waves = vect(1:2);
81                  circuit_array(next-1).Vou     = vect(3);
82                  next = index-1;
83              end
84
85              %solving circuit: propagating saw waves
86              for i=1:length(circuit_array)-1
87                  M = circuit_array(i).Tn;
88                  circuit_array(i).O_Waves = linsolve(M, circuit_array(
    i).I_Waves);
89                  circuit_array(i+1).I_Waves = circuit_array(i).O_Waves
    ;
90              end
91              M = circuit_array(length(circuit_array)).Tn;
92              circuit_array(length(circuit_array)).O_Waves = linsolve(M
    , circuit_array(length(circuit_array)).I_Waves);
93              circuit_array(length(circuit_array)).O_Waves =
    circuit_array(length(circuit_array)).O_Waves.*[1;0];
```

```
94
95              %solving circuit: electrical ports computation
96              for i=1:length(circuit_array)
97                  cur = length(circuit_array)+1-i;
98                  M = [ circuit_array(cur).Tn, circuit_array(cur).Bn;
99                          circuit_array(cur).Cn, circuit_array(cur).
    t33n ]*[circuit_array(cur).O_Waves; circuit_array(cur).Vin];
100                 circuit_array(cur).I_Waves = M(1:2);
101                 circuit_array(cur).Vou = M(3);
102                 if cur == 1
103                     break
104                 else
105                     circuit_array(cur-1).O_Waves = M(1:2);
106                 end
107             end
108
109             circuit = circuit_array;
110
111         end
112
113         %generating simulation object
114         function Object = CreateSawObject(obj, type, params)
115             Object.Bn = [0;0];
116             Object.Cn = [0,0];
117             Object.t33n = 0;
118             Object.role = params.role;
119             Object.I_Waves = [0;0];
120             Object.O_Waves = [0;0];
121             Object.Vin = 0;
122             Object.Vou = 0;
123             switch type
124                 case 'G'
125                     Object.Tn = obj.gen_GratingMatrix(params.f,
    params.Nt, params.theta_ref);
126                 case 'T'
127                     T = obj.gen_IdtMatrix(params.f, params.Nt);
128                     Object.Tn = [T(1,1),T(1,2);T(2,1),T(2,2)];
129                     Object.Bn = [T(1,3);T(2,3)];
130                     Object.Cn = [T(3,1),T(3,2)];
131                     Object.t33n = T(3,3);
132                 case 'D'
133                     Object.Tn = obj.gen_Spacing(params.f, params.
    dist_type, params.Ls);
134             end
135         end
136
137         %generating IDT transmission matrix
138         function T = gen_IdtMatrix(obj, f, Nt)
```

```
139             t0 = obj.Ga(Nt,f)*(obj.idt.Rs+obj.idt.Ze)/(1+1j*obj.
    ThetaE(Nt,f));
140             t13 = sqrt(2*obj.Ga(Nt,f)*obj.idt.Ze)/(1+1j*obj.ThetaE(Nt
    ,f))*exp(1j*obj.ThetaT(Nt,f)/2);
141             t33 = 1 -(2j*obj.ThetaC(Nt,f))/(1+1j*obj.ThetaE(Nt,f));
142             s = (-1)^Nt;
143             T = [s*(1+t0)*exp(1j*obj.ThetaT(Nt,f)), -s*t0
                        , t13;
144                  s*t0                                    ,  s*(1-t0)*exp(-1j
    *obj.ThetaT(Nt,f)), t13*exp(-1j*obj.ThetaT(Nt,f));
145                  s*t13                                   , -s*t13*exp(-1j*
    obj.ThetaT(Nt,f))    , t33];
146         end
147         %generating grating transmission matrix at f
148         function G = gen_GratingMatrix(obj, f, Nt, theta_ref)
149             sigma = sqrt(obj.idt.k12^2-(obj.delta(f)-1j*obj.material.
    loss)^2);
150             L = Nt*obj.material.lambdaS/2;
151             C = (obj.idt.k12/sigma)*cosh(sigma*L);
152             G(1,1) = (sigma/obj.idt.k12+1j*(obj.delta(f)-1j*obj.
    material.loss)/obj.idt.k12*tanh(sigma*L))*exp( 1j*obj.material.
    beta*L);
153             G(2,2) = (sigma/obj.idt.k12-1j*(obj.delta(f)-1j*obj.
    material.loss)/obj.idt.k12*tanh(sigma*L))*exp(-1j*obj.material.
    beta*L);
154             G(1,2) =  1j*exp(-1j*theta_ref)*tanh(sigma*L)*exp(1j*obj.
    material.beta*L);
155             G(2,1) = -1j*exp(1j*theta_ref)*tanh(sigma*L)*exp(-1j*obj.
    material.beta*L);
156             G = C*G;
157         end
158         %generating Spacing transmission matrix
159         function D = gen_Spacing(obj, f, dist_type, Ls)
160             beta =  2*pi/obj.material.Vs*f;
161             if dist_type == "time"
162                 L = Ls*obj.material.Vs;
163             else
164                 L = Ls;
165             end
166             D = [ exp(1j*beta*L), 0; 0, exp(-1j*beta*L)];
167         end
168         %Internal functions
169
170
171
172         function value = Ct(obj, N)
173             value = (N-1)/2*obj.idt.Cs;
174         end
175
```

```
176         function value = delta(obj, f)
177             value = 2*pi*(f-obj.f0)/obj.material.Vs+obj.idt.k11;
178         end
179 
180         function value = ThetaT(obj, Nt,f)
181             value = Nt*obj.material.lambdaS*obj.delta(f)*0.5;
182         end
183 
184         function value = ThetaC(obj, Nt,f)
185             value = 2*pi*f*obj.Ct(Nt)*(obj.idt.Rs+obj.idt.Ze);
186         end
187 
188         function value = Ga(obj, Nt,f)
189             value = obj.idt.G0*(Nt-1)^2*(sin(obj.ThetaT(Nt,f)/2)/(obj
    .ThetaT(Nt,f)/2))^2;
190         end
191 
192         function value = Ba(obj, Nt,f)
193             value = obj.idt.G0*2*(Nt-1)^2*(sin(obj.ThetaT(Nt,f))-obj.
    ThetaT(Nt,f))/(obj.ThetaT(Nt,f))^2;
194         end
195 
196         function value = ThetaE(obj, Nt,f)
197             value = (2*pi*f*obj.Ct(Nt)+obj.Ba(Nt,f))*(obj.idt.Rs+obj.
    idt.Ze);
198         end
199     end
200 end
```

This code is used to analyze the experimental results

content/code/misure_sensore.m

```
1  clear all
2  close all
3  clc
4 
5  %misure sperimentali
6  load matlab.mat
7 
8  alpha = 0.004; % fattore di variazione lineare della resistenza PT100
       con T
9  R0 = 100; % valore PT100 a 0 C
10 Rr = 50; % impedenza di riferimento
11 s11 = 0.291736781+1j*0.14887587699999999; %valori misurati dal DUT
12 s21 = 0.62433093699999997+1j*0.091971114000000007;%valori misurati
       dal DUT
13 temp = linspace(-10,310,320); % range di temperatura
14 
15 %curva teorica
```

```
for i=1:320
    RL = R0*(1+alpha*(temp(i)));
    gL = (RL-Rr)/(RL+Rr);
    gamma11_nt(i) = s11+(s21^2*gL)/(1-gL*s11);
end
%curva teorica con offset, riduce l'errore relativo al minimo valore
%possibile
errore = 1;
for q_corr=-1.6:0.1:1.6
    for offset=90:200
        for i=1:320
            RL = R0*(1+alpha*(temp(i)-offset));
            gL = (RL-Rr)/(RL+Rr);
            gamma11(i) = s11+(s21^2*gL)/(1-gL*s11);
        end
        curva_teorica = 20*log10(abs(gamma11))+q_corr;
        c_err = calcolo_errore(curva_teorica, yMeas, xMeas);
        if c_err<= errore
            errore = c_err;
            q_f = q_corr;
            o_f = offset;
            RLc = curva_teorica;
        end
    end
end


%curva a bassa temperatura
[p_low,S] = polyfit(xMeas(1:13),yMeas(1:13),1);
[y_reg_low, delta_l] = polyval(p_low,temp,S);
%curva ad alta temperatura
[p_high,S] = polyfit(xMeas(14:25),yMeas(14:25),1);
[y_reg_high, delta_h] = polyval(p_high,temp,S);

figure(1);
plot( temp, 20*log10(abs(gamma11_nt)),'--b' );
hold on
plot( temp, RLc, '--c' );
hold on
plot( xMeas, yMeas, '*r' );
%traccia punti sperimentali
for i=1:25
    for j=1:35
        plot(xMeas(i),vecMeas(i,j),'dg');
        hold on
    end
end
hold on
plot( xMeas, yMeas, '*r' );
```

```
65 hold on
66 ylim([-11 0])
67 xlim([0 310])
68 xlabel("Temperature [ C ]")
69 ylabel("Return Loss [dB]")
70 legend('S_{11} computed','S_{11} computed with offset','Averaged
       values','Experimental values')
71
72 figure(2)
73 plot( temp, RLc,'--c' );
74 hold on
75 plot( xMeas, yMeas, '*r' );
76 hold on
77 plot( temp, y_reg_low );
78 hold on
79 plot( temp, y_reg_high);
80 hold on
81 ylim([-11 0])
82 xlim([0 310])
83 xlabel("Temperature [ C ]")
84 ylabel("Return Loss [dB]")
85 legend('S_{11} computed with offset','Averaged values','S_{11} low
       temp. line','S_{11} high temp. line')
86
87 figure(3)
88
89 [p_q,S] = polyfit(xMeas,yMeas,2);
90 [y_regq, delta] = polyval(p_q,temp,S);
91
92 plot( temp, RLc,'--c' );
93 hold on
94 plot( xMeas, yMeas, '*r' );
95 hold on
96 plot(temp, y_regq, temp,y_regq+2*delta,'m--',temp,y_regq-2*delta,'m--
       ');
97 hold on
98
99 ylim([-11 0])
100 xlim([0 310])
101 xlabel("Temperature [ C ]")
102 ylabel("Return Loss [dB]")
103 legend('S_{11} computed with offset','Averaged values','S_{11}
       quadratic approximation','Prediction interval 95%')
104 %
105 %
106 % %stampa coefficienti rette e curve
107 %retta di regressione full temperature range
108 [p_lin,S] = polyfit(xMeas,yMeas,1);
109 [y_reg_lin, delta_lin] = polyval(p_lin,temp,S);
```

```
110
111 %stampo i risultati ottenuti
112 fprintf('Errore relativo massimo rispetto alla curva teorica : %f \n'
        , calcolo_errore(RLc, yMeas, xMeas))
113 fprintf('Coefficienti rette di regressione\n Low  temp: m = %f \t q =
        %f\n High temp: m = %f \t q = %f\n',p_low(1),p_low(2),p_high(1),
        p_high(2))
114 fprintf('Coefficiente retta di regressione\n Full range: m = %f \t q
        = %f\n',p_lin(1),p_lin(2))
115 fprintf('Errore relativo massimo Low temp : %f \n', calcolo_errore(
        y_reg_low, yMeas(1:13), xMeas(1:13)))
116 fprintf('Errore relativo massimo High temp : %f \n', calcolo_errore(
        y_reg_high, yMeas(14:25), xMeas(14:25)))
117 fprintf('Errore relativo massimo Full temp : %f \n', calcolo_errore(
        y_reg_lin, yMeas, xMeas))
118 fprintf('Coefficienti parabola approssimante\n a = %f\t b=%f\t c=%f\n
        ',p_q(1),p_q(2),p_q(3))
119 fprintf('Errore relativo massimo parabola : %f \n', calcolo_errore(
        y_regq, yMeas, xMeas))
120
121
122 function errore_r = calcolo_errore(funzione, y_misure, x_misure)
123     for i=1:length(x_misure)
124         x = x_misure(i);
125         errori(i) = abs(funzione(x+10)-y_misure(i))/abs(funzione(x
        +10));
126         i = i+1;
127     end
128     errore_r = max(errori);
129 end
```

The program IDT MASK ELEMENT GENERATOR have been developed in python the code is shown below:

content/code/application.py

```
1 from tkinter import *
2 from tkinter import filedialog
3 from tkinter import messagebox
4 from PIL import ImageTk,Image
5 import os
6 import math
7
8 class MaskGenerator:
9
10
11     def on_closing():
12         print("bye")
13         exit(0)
```

```
14
15      def __init__(self):
16
17          self.App = Tk()
18          self.App.title("IDT MASK ELEMENT GENERATOR")
19
20          self.lambdaS = StringVar()
21          self.a = StringVar()
22          self.b = StringVar()
23          self.W = StringVar()
24          self.W_off = StringVar()
25
26          self.lambdaS.set("0")
27          self.a.set("0")
28          self.b.set("0")
29          self.W.set("80")
30          self.W_off.set("50")
31
32          self.FrameBasicParam()
33          self.FrameDeviceParam()
34
35          Label(self.App, text="Basic parameters configuration").pack()
36          self.frm1.pack()
37
38          #first frame image
39          canvas = Canvas(self.App, width = 300, height = 140)
40          canvas.pack()
41          img = ImageTk.PhotoImage(Image.open("immagine.png").resize
    ((300,130)))
42          canvas.create_image(20, 20, anchor=NW, image=img)
43
44          Label(self.App, text="Device configuration").pack()
45          self.frm2.pack()
46
47          canvas1 = Canvas(self.App, width = 450, height = 160)
48          canvas1.pack()
49          img1 = ImageTk.PhotoImage(Image.open("sensors.png").resize
    ((400,130)))
50          canvas1.create_image(20, 20, anchor=NW, image=img1)
51
52
53          self.App.mainloop()
54
55      def setBasics(self):
56          freq = float(self.ent_f0.get())
57          lmb = round(3488.0/(freq*1000000)*1e6,2)
58          self.lambdaS.set(str(lmb))
59          self.a.set(str(lmb/4))
60          self.b.set(str(lmb/2))
```

```
61
62      def FrameBasicParam(self):
63
64          self.frm1 = Frame( relief="sunken", borderwidth=1 )
65          lbl_f0 = Label(self.frm1, text="Insert f0 [MHz]")
66          self.ent_f0 = Entry(self.frm1, width=10, textvariable=
    StringVar(self.frm1,value=str(100)))
67
68          lbl_L = Label(self.frm1, text="lambda SAW")
69          self.ent_L = Entry(self.frm1, width=10, textvariable=self.
    lambdaS)
70          lbl_a = Label(self.frm1, text="a")
71          self.ent_a = Entry(self.frm1, width=10, textvariable=self.a)
72          lbl_b = Label(self.frm1, text="b")
73          self.ent_b = Entry(self.frm1, width=10, textvariable=self.b)
74          lbl_W = Label(self.frm1, text="W unit of lambdaS")
75          self.ent_W = Entry(self.frm1, width=10, textvariable=self.W)
76          lbl_Wf = Label(self.frm1, text="W offset unit of lambdaS")
77          self.ent_Wf = Entry(self.frm1, width=10, textvariable=self.
    W_off)
78
79          button = Button(self.frm1, text="Apply params",command=self.
    setBasics)
80
81          lbl_f0.grid(row=1,column=1)
82          self.ent_f0.grid(row=1,column=2)
83          lbl_L.grid(row=1,column=3)
84          self.ent_L.grid(row=1,column=4)
85
86          lbl_a.grid(row=2,column=1)
87          self.ent_a.grid(row=2,column=2)
88          lbl_b.grid(row=3,column=1)
89          self.ent_b.grid(row=3,column=2)
90          lbl_W.grid(row=2,column=3)
91          self.ent_W.grid(row=2,column=4)
92          lbl_Wf.grid(row=3,column=3)
93          self.ent_Wf.grid(row=3,column=4)
94
95          button.grid(row=4,column=2)
96
97      def GenIDT(self, N_pair, a, b, offset, W, x, mask_file ):
98          for i in range(0,N_pair):
99              mask_file.write("B "+str(a*10)+" "+str((W+offset)*10)+" "
    +str(x*10)+" 0;\n")
100             mask_file.write("B "+str(a*10)+" "+str((W+offset)*10)+" "
    +str((x+b)*10)+" "+str(offset*10)+";\n")
101             x += b+2*a
102         return x
103
```

```
104     def GenGrating(self, N_pair, a, b, offset, W, x,mask_file ):
105         for i in range(0,N_pair):
106             mask_file.write("B "+str(a*10)+" "+str(W*10)+" "+str(x
    *10)+" "+str(offset*5)+";\n")
107             mask_file.write("B "+str(a*10)+" "+str(W*10)+" "+str((x+b
    )*10)+" "+str(offset*5)+";\n")
108             x += b+2*a
109         return x
110 
111     def genMask(self):
112         #getting params
113         lambdaP = int(round(float(self.ent_L.get())))
114         a = int(round(float(self.ent_a.get())))
115         b = int(round(float(self.ent_b.get())))
116         offset = int(round(float(self.ent_Wf.get()))*lambdaP)
117         D = int(round(float(self.ent_D.get()))*lambdaP)
118         Dg = int(round(float(self.ent_S.get()))*lambdaP)
119         W = int(round(float(self.ent_W.get()))*lambdaP)
120 
121         N_in = int(self.ent_Nin.get())
122         N_ou = int(self.ent_Nou.get())
123         N_gr = int(self.ent_G.get())
124 
125         header = open("header_file.txt")
126         mask_file = open("output.cif","w+")
127         footer = open("footer_file.txt")
128         #opening file
129         for line in header:
130             mask_file.write(line)
131         x=0
132         #generating file
133 
134         line_elements = self.ent_file.get().split(" ")
135         x_i = []
136         x_f = []
137         x_t = []
138         for obj in line_elements:
139             if obj == "G":
140                 x = self.GenGrating( N_gr, a, b, offset, W, x,
    mask_file )
141             elif obj == "Gs":
142                 x_i.append(x)
143                 x = self.GenGrating( N_gr, a, b, offset, W, x,
    mask_file )
144                 x_f.append(x)
145                 x_t.append(0)
146             elif obj == "S":
147                 x = x+Dg
148             elif obj == "IN":
```

```
149                 x_i.append(x)
150                 x = self.GenIDT( N_in, a, b, offset, W,  x,mask_file
    )
151                 x_f.append(x)
152                 x_t.append(1)
153             elif obj == "D":
154                 x = x+D
155             elif obj == "OU":
156                 x_i.append(x)
157                 x = self.GenIDT( N_ou, a, b, offset, W,  x,mask_file
    )
158                 x_f.append(x)
159                 x_t.append(2)
160             else:
161                 print("Error")
162                 break
163         x_end = x
164         for i in range(0,len(x_i)):
165             width = x_f[i]-x_i[i]
166             #drawing connections
167             mask_file.write("B "+str((width)*10)+" "+str((100)*10)+"
    "+str(round(x_i[i]+width/2)*10)+" "+str(round((W+3*offset)/2)*10)+
    ";\n")
168             mask_file.write("B "+str((width)*10)+" "+str((100)*10)+"
    "+str(round(x_i[i]-a+width/2)*10)+" "+str(-round((W+offset)/2)*10)
    +";\n")
169             #drawing wires2connections
170             if x_t[i] == 0:
171                 pass
172             elif x_t[i] == 1:
173                 width = x_i[i]
174                 mask_file.write("B "+str((width+300)*10)+" "+str
    ((100)*10)+" "+str(round(-100+width/2)*10)+" "+str(round((W+3*
    offset)/2)*10)+";\n")
175                 mask_file.write("B "+str((width+300)*10)+" "+str
    ((100)*10)+" "+str(round(-a+width/2)*10)+" "+str(-round((W+offset)
    /2)*10)+";\n")
176                 mask_file.write("B "+str((2000)*10)+" "+str((2000)
    *10)+" "+str((-1000-100)*10)+" "+str(round((W+3*offset)/2)*10)+";\
    n")
177                 mask_file.write("B "+str((2000)*10)+" "+str((2000)
    *10)+" "+str((-1000-100)*10)+" "+str(-round((W+offset)/2)*10)+";\n
    ")
178             elif x_t[i] == 2:
179                 width = x_end-x_f[i]
180                 mask_file.write("B "+str((width+300)*10)+" "+str
    ((100)*10)+" "+str(round(100+x_f[i]+width/2)*10)+" "+str(round((W
    +3*offset)/2)*10)+";\n")
```

```
181                 mask_file.write("B "+str((width+300)*10)+" "+str
    ((100)*10)+" "+str(round(-100+x_f[i]-a+width/2)*10)+" "+str(-round
    ((W+offset)/2)*10)+";\n")
182                 mask_file.write("B "+str((2000)*10)+" "+str((2000)
    *10)+" "+str((x_end+1000+100)*10)+" "+str(round((W+3*offset)/2)
    *10)+";\n")
183                 mask_file.write("B "+str((2000)*10)+" "+str((2000)
    *10)+" "+str((x_end+1000+100)*10)+" "+str(-round((W+offset)/2)*10)
    +";\n")
184             else:
185                 pass
186
187         #closing file
188         for line in footer:
189             mask_file.write(line)
190
191         footer.close()
192         header.close()
193         mask_file.close()
194
195     def FrameDeviceParam(self):
196         self.frm2 = Frame( relief="sunken", borderwidth=1 )
197
198         lbl_Nin = Label(self.frm2, text="input IDT pairs (IN)")
199         self.ent_Nin = Entry(self.frm2, width=10, textvariable=
    StringVar(self.frm2,value=str(15)))
200
201         lbl_Nou = Label(self.frm2, text="output IDT pairs (OU)")
202         self.ent_Nou = Entry(self.frm2, width=10, textvariable=
    StringVar(self.frm2,value=str(15)))
203         lbl_G = Label(self.frm2, text="IDT grating (G)")
204         self.ent_G = Entry(self.frm2, width=10, textvariable=
    StringVar(self.frm2,value=str(60)))
205         lbl_D = Label(self.frm2, text="Delay unit of lambdaS (D)")
206         self.ent_D = Entry(self.frm2, width=10, textvariable=
    StringVar(self.frm2,value=str(100)))
207         lbl_S = Label(self.frm2, text="Spacer unit of lambdaS (S)")
208         self.ent_S = Entry(self.frm2, width=10, textvariable=
    StringVar(self.frm2,value=str(3.6)))
209         lbl_file = Label(self.frm2, text="Device Structure")
210         self.ent_file = Entry(self.frm2, width=20, textvariable=
    StringVar(self.frm2,value="G S IN D OU S G"))
211
212         button = Button(self.frm2, text="Generate file",command=self.
    genMask)
213
214         lbl_Nin.grid(row=1,column=1)
215         self.ent_Nin.grid(row=1,column=2)
216         lbl_Nou.grid(row=1,column=3)
```

```
217             self.ent_Nou.grid(row=1,column=4)
218
219             lbl_G.grid(row=2,column=1)
220             self.ent_G.grid(row=2,column=2)
221             lbl_D.grid(row=2,column=3)
222             self.ent_D.grid(row=2,column=4)
223
224             lbl_S.grid(row=3,column=1)
225             self.ent_S.grid(row=3,column=2)
226
227             lbl_file.grid(row=4,column=1)
228             self.ent_file.grid(row=4,column=2)
229             button.grid(row=6, column=2)
230
231 test = MaskGenerator()
```

Bibliography

[1] R. M White and F. W Voltmer. «DIRECT PIEZOELECTRIC COUPLING TO SURFACE ELASTIC WAVES». In: *Applied physics letters* 7.12 (1965), pp. 314–316. ISSN: 0003-6951 (cit. on pp. 2, 4).

[2] L Reindl, G Scholl, T Ostertag, H Scherr, U Wolff, and F Schmidt. «Theory and application of passive SAW radio transponders as sensors». In: *IEEE transactions on ultrasonics, ferroelectrics, and frequency control* 45.5 (1998), pp. 1281–1292. ISSN: 0885-3010 (cit. on p. 4).

[3] Colin K Campbell. «Surface acoustic wave devices for mobile and wireless communications». In: *Surface acoustic wave devices for mobile and wireless communications*. Applications of modern acoustics. San Diego: Academic press, 1998. Chap. 2 (cit. on pp. 5–7).

[4] Kerstin Länge. «Bulk and Surface Acoustic Wave Sensor Arrays for Multi-Analyte Detection: A Review». In: *Sensors (Basel, Switzerland)* 19.24 (2019), p. 5382. ISSN: 1424-8220 (cit. on p. 5).

[5] Sapna Tyagi and Varde G. Mahesh. «SAW AND INTERDIGITAL TRANSDUCERS». In: *International Journal of Scientific Engineering Research* 3.12 (2012), pp. 1141–1144. ISSN: 2229-5518 (cit. on pp. 8, 9).

[6] Haekwan Oh, Keekeun Lee, Kyoungtae Eun, Sung-Hoon Choa, and Sang Yang. «Development of a high-sensitivity strain measurement system based on a SH SAW sensor». In: *Journal of Micromechanics and Microengineering - J MICROMECHANIC MICROENGINEER* 22.2 (2012), p. 025002. ISSN: 0960-1317 (cit. on p. 8).

[7] *Bragg's law*. Mar. 2021. URL: `https://en.wikipedia.org/wiki/Bragg's_law` (cit. on p. 8).

[8] Colin K Campbell. «Surface acoustic wave devices for mobile and wireless communications». In: *Surface acoustic wave devices for mobile and wireless communications*. Applications of modern acoustics. San Diego: Academic press, 1998. Chap. 11 (cit. on pp. 10, 11).

[9] Colin K Campbell. «Surface acoustic wave devices for mobile and wireless communications». In: *Surface acoustic wave devices for mobile and wireless*

communications. Applications of modern acoustics. San Diego: Academic press, 1998. Chap. 3 (cit. on pp. 12–17).

[10] Colin K Campbell. «Surface acoustic wave devices for mobile and wireless communications». In: *Surface acoustic wave devices for mobile and wireless communications*. Applications of modern acoustics. San Diego: Academic press, 1998. Chap. 4 (cit. on pp. 12, 18–22, 27).

[11] Colin K Campbell. «Surface acoustic wave devices for mobile and wireless communications». In: *Surface acoustic wave devices for mobile and wireless communications*. Applications of modern acoustics. San Diego: Academic press, 1998. Chap. 9 (cit. on pp. 12, 23–25).

[12] Colin K Campbell. «Surface acoustic wave devices for mobile and wireless communications». In: *Surface acoustic wave devices for mobile and wireless communications*. Applications of modern acoustics. San Diego: Academic press, 1998. Chap. 11.7 (cit. on pp. 12, 28–32, 38).

[13] Colin K Campbell. «Surface acoustic wave devices for mobile and wireless communications». In: *Surface acoustic wave devices for mobile and wireless communications*. Applications of modern acoustics. San Diego: Academic press, 1998. Chap. 11 (cit. on p. 31).

[14] *Radar*. Mar. 2021. URL: `https://en.wikipedia.org/w/index.php?title=Radar&oldid=1030047095` (cit. on p. 69).